BURST PRESSURE PREDICTION OF COLLINEAR CRACK IN STEEL PIPELINE.

MUHAMMAD ALIF HAFIZ BIN ABD MURAD

Report submitted in partial fulfillment of the requirements
for the award of the degree of Bachelor of Mechanical Engineering

Faculty of Mechanical Engineering
UNIVERSITI MALAYSIA PAHANG

JUNE 2013

UNIVERSITI MALAYSIA PAHANG

BORANG PENGESAHAN STATUS TESIS♦

JUDUL: **BURST PRESSURE PREDICTION OF COLLINEAR CRACK IN STEEL PIPELINE**

SESI PENGAJIAN: 2012/2013

Saya   **MUHAMMAD ALIF HAFIZ BIN ABD MURAD (900108-07-5279)**

mengaku membenarkan tesis (Sarjana Muda/~~Sarjana~~ /~~Doktor Falsafah~~)* ini disimpan di Perpustakaan dengan syarat-syarat kegunaan seperti berikut:

1. Tesis adalah hakmilik Universiti Malaysia Pahang (UMP).
2. Perpustakaan dibenarkan membuat salinan untuk tujuan pengajian sahaja.
3. Perpustakaan dibenarkan membuat salinan tesis ini sebagai bahan pertukaran antara institusi pengajian tinggi.
4. **Sila tandakan (√)

☐	**SULIT**	(Mengandungi maklumat yang berdarjah keselamatan atau kepentingan Malaysia seperti yang termaktub di dalam AKTA RAHSIA RASMI 1972)
☐	**TERHAD**	(Mengandungi maklumat TERHAD yang telah ditentukan oleh organisasi/badan di mana penyelidikan dijalankan)
√	**TIDAK TERHAD**	

Disahkan oleh:

_____   _____
(TANDATANGAN PENULIS)   (TANDATANGAN PENYELIA)

Alamat Tetap:

NO. 10, LRG SERI DAMAI BARU 27,   NORHAIDA BINTI ABD RAZAK
TMN ALAM IMPIAN,   (Nama Penyelia)
25150 KUANTAN,
PAHANG.

Tarikh: 26 JUN 2013   Tarikh: : 26 JUN 2013

CATATAN: *   Potong yang tidak berkenaan.
                  **   Jika tesis ini SULIT atau TERHAD, sila lampirkan surat daripada pihak
                            berkuasa/organisasi berkenaan dengan menyatakan sekali tempoh tesis ini perlu
                            dikelaskan sebagai atau TERHAD.
                  ♦   Tesis dimaksudkan sebagai tesis bagi Ijazah doktor Falsafah dan Sarjana secara
                            Penyelidikan, atau disertasi bagi pengajian secara kerja kursus dan
                            penyelidikan, atau Laporan Projek Sarjana Muda (PSM).

UNIVERSITI MALAYSIA PAHANG

FACULTY OF MECHANICAL ENGINEERING

I certify that the project entitled *"Burst Pressure Prediction of Collinear Crack in Steel Pipeline"* is written by *Muhammad Alif Hafiz Bin Abd Murad*. I have examined the final copy of this report and in my opinion, it is fully adequate in terms of language standard, and report formatting requirement for the award of the degree of Bachelor Engineering. I herewith recommend that it be accepted in partial fulfillment of the requirements for the degree of Bachelor Mechanical Engineering.

DR. YULI PANCA ASMARA

Examiner   Signature

SUPERVISOR'S DECLARATION

I hereby declare that I have checked this project and in my opinion, this project is adequate in terms of scope and quality for the award of the degree of Bachelor of Mechanical Engineering.

Signature   :
Name of Supervisor   : MRS. NORHAIDA BINTI ABD RAZAK
Position   : LECTURER
Date   : 26th June 2013

STUDENT'S DECLARATION

I declare that this report titled *"Burst Pressure Prediction of Collinear Crack in Steel Pipeline"* is my result of my own research except as stated in the references. The project has not been accepted for any degree and is not concurrently submitted for award of other degree.

Signature   :

Name   : MUHAMMAD ALIF HAFIZ BIN ABD MURAD

ID Number   : MA09045

Date   : 26th June 2013

IN THE NAME OF ALLAH,
THE MOST BENEFICENT, THE MOST MERCIFUL

A special dedication of this grateful feeling to my
beloved parents, En.Abd Murad Bin Ab. Ghani and Pn.Radzarah Bt. Moktar
for giving me full of love and moral support. It is very meaningful to me in order to
finish up my degree's study. Last but not least to all my colleagues and my lovely
friends.

Thanks for all the support, wishes and love.

ACKNOWLEDGEMENT

First of all, I would like to express my highest gratitude to Allah the Almighty for blessing me in finishing this project. Alhamdulillah with the permission of Allah the Most High and who has given me His guidance and facilitate me to do what I can. I have been trying to get this thesis with the language simple, clear and easy to understand for all levels of society.

I am grateful and would like to express my sincere gratitude and deepest appreciation to my supervisor Mrs. Norhaida binti Abd Razak for her germinal ideas, invaluable guidance, continuous encouragement and constant support in making this thesis. This thesis could not been done without her who not only served as my supervisor but also encourage me throughout the process. I appreciate her consistent support from the first day I applied to graduate program to these concluding moments. I am truly grateful for her progressive vision about my training in science, her tolerance of my naive mistakes, and her commitment to my future career.

Besides that, I would like to acknowledge with much appreciation the crucial role of the staff at Analysis Room Faculty of Mechanical, for their valuable comments, sharing their time and knowledge on this research project during the project was carried out and giving a permission to use all the necessary tools in the laboratory. They have contributed towards my understanding and thoughts.

Last but not least, an expression of thanks is extended to everyone who has offered their help and support especially to my family and friends. All of their helps are very significant to the success of this project. I cannot find the appropriate words that could properly describe my appreciation for their devotion, support and faith in my ability to attain my goal.

ABSTRACT

The predictions of pipeline burst pressure in the early stage are very importance in order to provide assessment for future inspection and maintenances activities. The failures of pipelines contribute to economic implications, fatal injuries and also constitute serious hazards to the environment due to leakage. This project is a study on interaction effect of the distance between cracks for material grade B steel pipe using finite element analysis (FEA). The objectives for this project are to study the interaction of two linear cracks and analyze the maximum pressure defect for various distances between crack and crack length. This project include the analysis of the material grade B steel by using MSC Patran 2008 r1 software as pre-processor and MSC Marc 2008 r1 software as a solver. This analysis investigates one failure criterions that is von Mises stress as to predict the failure of defective pipe. Half of pipe was simulated by applying the symmetrical condition. The pipe is modeled in 3D with outer diameter of 60.5 mm, wall thickness of 4 mm and different defect parameters. Result shows that the maximum pressure increases when the distance between cracks increase and the crack length decrease. The results have been compared to available design codes for corroded pipelines such as ASME B31G, Modified ASME B31G and DNV RP F101. The comparison with design codes have shown that FEA burst pressure gives higher values.

ABSTRAK

Ramalan-ramalan tekanan letus saluran paip di peringkat awal adalah sangat penting untuk menyediakan penilaian bagi pemeriksaan pada masa akan datang dan aktiviti penyelenggaraan. Kegagalan saluran paip minyak dan gas menyumbang kepada implikasi ekonomi, kecederaan maut dan juga merupakan suatu bahaya yang serius kepada alam sekitar yang berpunca daripada kebocoran. Projek ini adalah bertujuan untuk mengkaji kesan hubungan rekahan ke atas besi gred B dengan menggunakan perisian (FEA). Objektif untuk kajian ini adalah untuk mengkaji interaksi di antara dua rekahan yang selari dan untuk mengkaji tekanan tertinggi ke atas perbezaan jarak antara rekahan dan tekanan ke atas panjang rekahan. Projek ini melibatkan analisa besi gred B dengan menggunakan perisian MSC Patran 2008 r1 sebagai pra-pemproses dan MSC Marc 2008 perisian r1 sebagai penyelesai. Didalam analisis ini, satu kriteria kegagalan iaitu tekanan von Mises digunakan untuk meramalkan kegagalan paip rosak. Separuh daripada paip disimulasi dengan menggunakan keadaan simetri. Paip dimodel dalam bentuk 3D dengan diameter luar 60.5 mm, ketebalan dinding 4 mm dan parameter kecacatan yang berbeza. Keputusan menunjukkan bahawa tekanan yang pecah meningkat apabila jarak antara rekahan menigkat dan panajang rekahan berkurang. Keputusan telah berbanding kod reka bentuk tersedia untuk saluran paip berkarat seperti ASME B31G, Modified ASME B31G dan DNV RP F101. Perbandingan dengan kod reka bentuk yang ada telah menunjukkan bahawa tekanan letus FEA memberikan nilai yang lebih tinggi.

TABLE OF CONTENTS

CHAPTER 3   METHODOLOGY

CHAPTER 4   RESULT AND DISCUSSION

CHAPTER 5   CONCLUSION AND RECOMMENDATION

REFERENCES
APPENDICES

LIST OF TABLES

LIST OF FIGURES

LIST OF SYMBOLS

t	Pipe thickness
d	Distance between cracks
$2c$	Crack length
σ_{UTS}	Ultimate tensile strength, MPa
σ_Y	0.2% offset yield strength, MPa
E	Young modulus
A_0	Cross-sectional area
L_0	Length
P	Pressure
K	Strain hardening coefficient
n	Strain hardening exponent
ν	Poisson's ratio
ε_f	Fracture strain
σ_e	Engineering stress
σ_t	True stress
ε_e	Engineering strain
ε_t	True strain
mm	Millimetre
MPa	Mega Pascal
%	Percent
kN	kilo Newton
Cu	Cuprum
H_2	Hydrogen
O_2	Oxygen

LIST OF ABBREVIATIONS

2D	Two Dimension
3D	Three Dimension
ASTM	American Society for Testing and Materials
ASME	American Society of Mechanical Engineers
API	American Petroleum Institute
ANSI	American National Standards Institute
DNV	Det Norske Veritas
FEA	Finite Element Analysis
FEM	Finite Element Method
HIC	Hydrogen Induced Cracking
RP	Recommended Practice
SCC	Stress Corrosion Cracking
SOHIC	Stress-Oriented Hydrogen Induced Cracking
MSS	Maximum Shear Stress
CSV	Comma-Separated Values
BC	Boundary Condition
CAD	Computer Aided Design

CHAPTER 1

INTRODUCTION

1.1 INTRODUCTION

This chapter will briefly explain about the introduction of this project. This chapter will consist of project background, problem statement, objectives, scope of study, and project flow chart. All this information is important before furthering to the analysis and study later.

1.2 PROJECT BACKGROUND

The increasing number of aging pipelines in operation is significantly increased the number of accidents such gas leaking and bursting pipeline. Failure due to corrosion defect has been major concern in maintaining pipeline integrity (Y.K. Lee et al., 2005). Most of the pipelines are allowed to operate after calculating the maximum internal or external product being transport. Accurate burst pressure prediction is important to structural the design and integrity assessment of the pipeline. The bursting of the pipe with wall thinning accompanies a bulge due to inelastic deformation at the wall. Therefore it is good to predict the burst pressure by considering the plastics deformation before bursting occur. The deformation characteristic is depending on the material and this study focus on material grade B. In this study, 3D elastic plastic FEA was conducted to examine the interaction between the distance between cracks and the cracks length on the failure pressure. Nonlinear finite element is used to analysed the interaction of multiple defect. The validity of the FEA was confirmed by comparing its result with industry models.

1.3 PROBLEM STATEMENT

Nowadays the increasing demand in oil and gas industry has influent the development of pipeline with the large diameter, thin in thickness, and made from high steel material so it can operate in high pressure. With increasing their age, the pipeline remaining strength depends on a few factors such operational condition, defect cause by construction, third party damage, corrosion and soil movement.

Corrosion is one of the defects in pipeline. The defect due to the corrosion at the pressurized pipeline can cause a high risk of failure and the pipe need to undergo the reliable assessment before it can be allowed to operate. Wall thinning caused by corrosion on the inner or outer surfaces of the pipelines will generate stress concentration on the pipe wall (Y.K. Lee et al., 2005). The highest stress and strain value will occur at the corrosion defect area, therefore the failure of the pipelines are usually expected at this location. Integrity assessment of corroded pipeline is very vital in oil and gas industry. Better understanding is required to reduce the conservatism involved in the current assessment method. There are many reliable assessment can be used to predict the burst pressure such ASME B31G, Modified ASME and DNV. Previous research has found out that finite element analysis has become a reliable engineering approach towards achieving actual results. Many consultant companies realize that it is difficult to have a finite element modeling of the offshore corroded pipeline as the modeling need further understanding and detail research on each data. In this research, finite element analysis will be implemented comparing with the available industry model as it is a higher demand in the oil and gas industry. This thesis will be a start and guidance in helping industries towards achieving accurate prediction of failure on defect pipelines.

1.4 OBJECTIVES

For this project, two main objectives are listed:

i. To determine the maximum pressure of defect pipe using finite element analysis (FEA).

ii. To study the interaction of the distance between two cracks.

iii. To compare the FEA results with the available design code such ASME B31G, Modified ASME B31G, and DNV-RP-F101.

1.5 SCOPE OF STUDY

This study was focused on the interaction of distance between two cracks in a pressurized pipeline. The scope consists of:

i. The geometry of the crack is rectangular cross section.

ii. The crack is at the outer surface of the pipeline.

iii. MSC Patran 2008 r1 software is used as pre-processor and MSC Marc 2008 r1 is used as solver to simulate the cracks.

iv. Material used is Material Grade B.

v. FEA results will be compared with the available design code such ASME B31G, Modified ASME B31G, and DNV-RP-F101.

1.6 PROJECT FLOW CHART

A flow chart is a graphical representation of a process. Each step in the process is represented by a different symbol and contains a short description of the process step. They are linked together with arrows showing the process flow direction. Flow chart is very important in doing research because it helping the viewer to understand and visualize the process flows. The terminology of work planning in this project is shown in Figure 1.1.
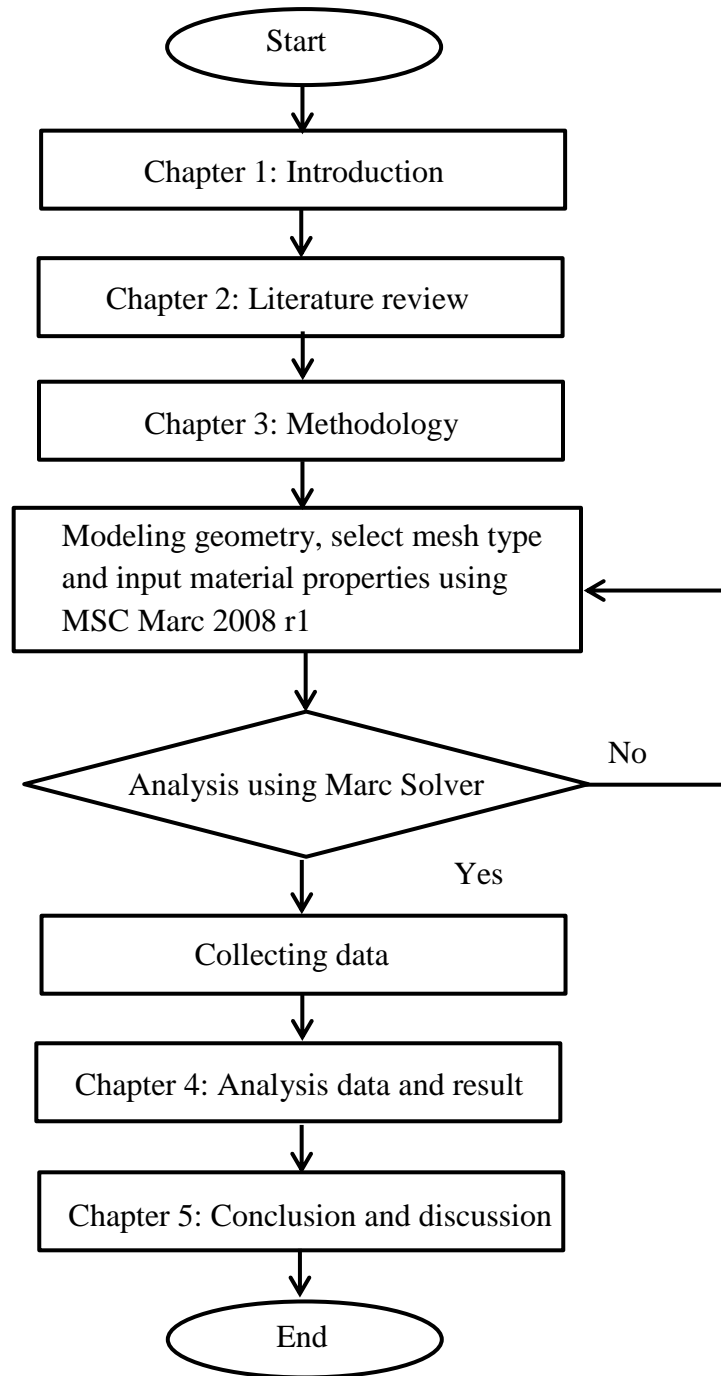
Figure 1.1: Project flow chart.

CHAPTER 2

LITERATURE REVIEW

2.1 INTRODUCTION

This chapter will briefly explain about the burst pressure model, material properties, type of defect, failure criteria and cause of failure in pipeline. The sources for this literature are taking from journals, articles, and books. Literature review is important to provide some information about previous research and help to facilitate when conducting this project. All this information is important to start the analysis and further study.

2.2 INTRODUCTION TO PIPELINE

Pipeline is a long pipe underground commonly used to transport oil and natural gas over long distances. For gases and liquids or any chemically stable substance can be sent through a pipeline. In general, pipelines can be classified in three categories depending on purpose that is gathering pipelines, transportation pipelines and distribution pipelines. Gathering pipelines is a group of smaller interconnected pipelines forming complex networks with the purpose of bringing crude oil or natural gas from several nearby wells to a treatment plant or processing facility (Kim et al., 2008). In this group, pipelines are usually short a couple of hundred meters and with small diameters. Also sub-sea pipelines for collecting product from deep water production platforms are considered gathering systems.

Transportation pipelines mainly long pipes with large diameters, moving products include oil, gas, and refined products between cities, countries and even continents. These transportation networks include several compressor stations in gas lines or pump stations for crude and multiproduct pipelines (Beaver and Thompson, 2006). Distribution pipelines composed of several interconnected pipelines with small diameters, used to take the products to the final consumer. Feeder pipelines were used to distribute gas to houses and business downstream.

2.3 MATERIAL PROPERTIES

2.3.1 Carbon Steel

Carbon steel is the most widely used engineering material in the overall of steel production worldwide (Morrow, 2010). Carbon steel can be defined as steel where the main interstitial alloying element is carbon. Carbon steel can be described as the structural material which is abundantly available, inexpensive, adequate formability and weldability, and has adequate mechanical properties but has a high general corrosion rate (Kadhim, 2011).

Although carbon steel is always related to the low corrosion resistance or high general corrosion rate, it is still the most widely used engineering material in this world. It is well known that carbon steel corrodes rapidly in seawater environment and requires adequate protection depending on the type of application. Though carbon steel is the most prone to corrosion, it is the least expensive of the most commonly perforated metals compared to other type of structural material. Carbon steel is used in large tonnages in marine applications, nuclear power and fossil fuel power plants, transportation, pipelines, mining, and construction (Kadhim, 2011).

2.3.2 Types of Carbon Steel

Carbon steel can be divided into five groups based on its carbon content which are low carbon steel, mild steel, medium carbon steel, high carbon steel and ultra-high carbon steel. Typical groups of carbon steels are tabulated in Table 2.1 and each group of carbon steel is provided with some examples which start with American Iron and Steel Institute (AISI). There are a total of five groups of carbon steel which shows different characteristics are discussed in Table 2.1. Different groups of carbon steel are applied in different application in worldwide and it depends on the characteristic of the carbon steel and the requirement of the application.

Table 2.1: Types of carbon steel.

Carbon steel types	Example AISI No.	% of carbon	Explanation
Low carbon steel	1010, 1012	0.05-0.15	It is neither ductile nor brittle. It is normally used when huge quantities of steel and high surface finish are required. It is used in the form of structural steel such as sheets, strips, rods and wires.
Mild steel	1018, 1020	0.16-0.29	Its price is usually low and it provides the material properties which are acceptable under many circumstances. It is characterized by a low tensile strength, but it is malleable, good machinability, and cheap. It is used to produce ship plates, welded turbines, boiler tubes and camshafts.
Medium carbon steel	1035, 1038	0.30-0.59	It is stronger and possesses better hardness and tensile strength but less ductility than mild steel. It has good machinability, deep hardening properties and fantastic wear resistance. It is used in automotive components which required higher strength such as stronger nut, large forgings, and high tensile tubes.
High carbon steel	1055	0.6-0.99	It is very strong, utilized in high-strength wires and springs. Ductility and machinability of steel decreases with the increase in carbon content. It is used in produce cold chisel, wrenches, jaws, hacksaw blades and railway service.
Ultra-high carbon steel		1-2	It could be tempered for greater hardness. It is utilized for special purposes such as non-industrial-purpose knives, punches or axles.

Source: Ashby and Johnson (2009)

2.3.3 Application of Carbon Steel in Seawater

Although carbon steel is highly related to the limited corrosion resistance compared to other common types of steels such as stainless steel, carbon steels are commonly used in seawater for structural applications such as ship hulls, offshore platforms, sheet piles and coastal facilities as well as seawater piping systems. All these applications required high corrosion resistance material since the medium environment of the applications is seawater which can increase the corrosion rate of the material (Kadhim, 2011). Basically, seawater in the ocean in the world has a salinity which is about 3.5 %. In other words, each litre by volume of seawater has approximately 35 grams of dissolved salts (predominantly sodium (Na^+) and chloride (Cl^-) ions).

Carbon steel is preferred in a seawater environment compared other types of material since carbon steel exhibit low initial cost compared with other materials, the ready availability of material and components and the existence of widely used and accepted welding procedures. However, the rate of corrosion of carbon steel is much higher and this becomes the main barrier of the usage of carbon steel in seawater environment. Basically, a system that produced or designed using carbon steel is much cheaper since carbon steel is inexpensive but the system is larger, heavier and shorter life compared to other structural material. Thus, the failures of the structure may occur earlier and it is within a few years and complete replacement is required compared to other better corrosion resistance structural material (Bennett, 2002).

However, in order to increase the corrosion resistance of carbon steel in seawater environment, method of coatings is largely applied. Coating is a famous and widely used method to protect the low corrosion resistance material such as plain carbon steel but it also increases the initial costs since more process is needed compared to plain carbon steel. Coating is applied on the both surfaces which are inner and outer surface in order to increase the corrosion resistance of the material. However, by applying a coating on the surface of the material, it introduces complications into the fabrication procedures, such as the need for a local removal prior to welding and re-application afterwards

(Morrow, 2010). Besides that, heat treated carbon steel can be used compared to plain carbon steel in order to improve the corrosion resistance of the carbon steel. Heat treated carbon steel has better mechanical properties and corrosion resistance compared to the plain carbon steel since different microstructure existed in the material.

2.4 CORROSION CONCEPTS

Corrosion can be defined as degradation of quality and properties in a material due to the chemical reaction between the components of the material and the surrounding during the electrochemical process (Iversen and Leffler, 2010). Electrochemical process is a general process which requires the presence of an anode, a cathode, an electrolyte, and an electrical circuit in order to active the reaction.

First, the metal at the anode is dissolved and the electrons are produced from the anode is shown in Figure 2.1. The number of electrons produced depends on the type of the metal used. After the electrons produced at the anode, the corrosion current is generated by the electrons and the electrons are transferred to the cathode through the electrolyte as a transfer medium. Equation (2.1) shows the general reaction that occurs at the anode (Iversen and Leffler, 2010).

$$M \longrightarrow Mn^+ + e^- \hspace{4cm} (2.1)$$
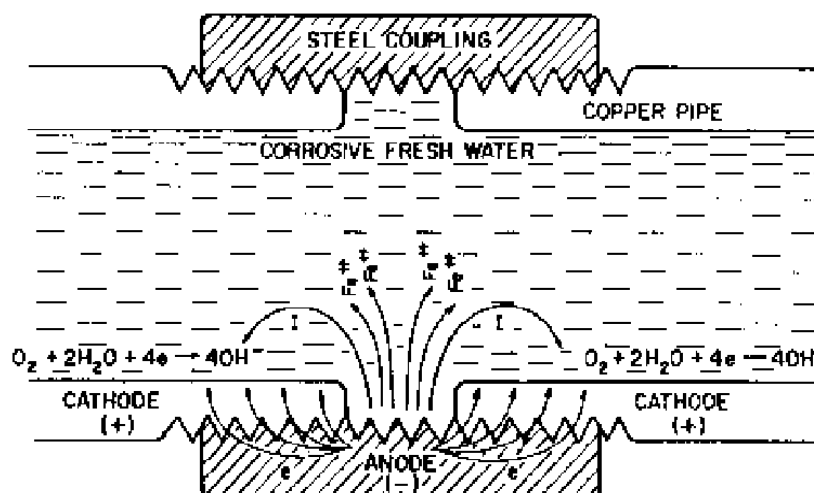
Figure 2.1: The basic corrosion cell.

Source: Iversen and Leffler (2010)

The reaction at the anode shows a loss of electrons, or oxidation is clearly shown in Figure 2.1. The electrons produced at the anode flow to the cathode through the electrolyte which initiates a reaction to occur at the cathode. The reaction in cathode depends on the medium of transfer which can be divided into three groups which are acidic solution, alkaline solution and neutral solutions. All of these reactions in each solution involve a gain of electrons and a reduction process which occurs at the cathode is shown in Equation (2.2) which in neutral solution. If the medium is in alkaline and neutral aerated solutions, the predominant cathodic reaction is shown in Equation (2.2) (Iversen and Leffler, 2010). The number of electrons produced at the anode must equal the number of electrons gained at the cathode since there can be no net gain or loss of electrons.

$$O_2 + 2H_2O + 4e^- \longrightarrow 4(OH^-) \hspace{3cm} (2.2)$$
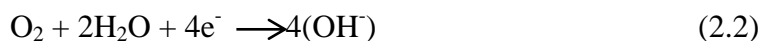
If Fe is placed at the anode which exposed to aerated, corrosive water, the anodic reaction is shown in Equation (2.3) which oxidation is occurred. However, at the cathode, reduction of oxygen is occurred as shown in Equation (2.1) (Iversen and

Leffler, 2010). Based on the Equation (2.3), two electrons are produced during the reaction at the anode. However, based on Equation (2.2), four electrons are required in order to balance the reaction at the cathode.

$$Fe \rightarrow Fe^{2+} + 2e^{-} \qquad (2.3)$$

Based on the concept of reaction, the number of electrons produced at the anode must equal the number of electrons gained at the cathode since the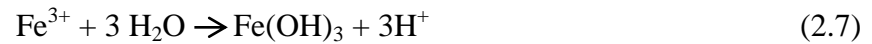re can be no net gain or loss of electrons. Thus, the anodic reaction is modified and shown as Equation (2.4) while the cathodic reactions would be similar to the previous equation (Iversen and Leffler, 2010). Finally, an overall oxidation-reduction reaction is shown in Equation (2.5) which summarized the oxidation-reduction reaction occurred at the cathode and anode.

$$2\ Fe \rightarrow 2Fe^{2+} + 4e^{-} \qquad (2.4)$$

$$2Fe + O_2 + 2H_2O \rightarrow 2Fe^{2+} + 4(OH^{-}) \qquad (2.5)$$

However, after the dissolution at anode, the ferrous ions or known as Fe2+ generally oxidize to ferric ions (Fe^{3+}) are shown in Equation (2.6) and these combine with hydroxide ions (OH^{-}) which formed at the cathode to give a corrosion product called iron oxide or in general term called as rust. There are several forms of rust which can be distinguished visually or by using spectroscopy. Basically rust consists of iron (III) oxides, Fe2O3·nH2O and iron (III) oxide-hydroxide, FeO(OH), or Fe(OH)$_3$ are shown in Equation (2.7) and (2.8). It can be concluded that anodic dissolution of metal occurs electrochemically while the insoluble corrosion products are formed by a secondary chemical reaction is shown in the equation below (Iversen and Leffler, 2010).

$$4Fe^{2+} + O_2 \rightarrow 4Fe^{3+} + 2\ O^{2-} \tag{2.6}$$

$$Fe^{3+} + 3\ H_2O \rightarrow Fe(OH)_3 + 3H^+ \tag{2.7}$$

$$Fe(OH)_3 \rightarrow FeO(OH) + H_2O \tag{2.8}$$

2.5 BURST PRESSURE MODEL

2.5.1 Introduction

The failure pressure prediction can be reduced by increasing corrosion depth and decrease of the steel grade. Besides that, the geometry of corrosion defects affects in the failure pressure prediction (Zhou and Huang, 2012) and other related factors such operational condition, defects occur during construction, third party damage and ground movement. Ground movement creates the longitudinal load thus produce the stress or strain condition to the pipe. For the loss of pipe wall thickness it means a reduction of pipeline structural intensity and that will increase the risk of failure. The maximum allowable operating pressure can be calculate for the defect pipe. There are five models which is known as industry model have been developed to calculate the failure pressure in corrosion defect pipe such ASME B31G, Modified ASME, DNV, RSTRENG and PCORCC (Zhou and Huang, 2012).

2.5.2 ASME B31G

American Society of Mechanical Engineers, ASME B31G was developed based on full scale burst test for defect pipes. This model is widely used in determining the remaining strength of the corroded pipeline (Xu and Cheng, 2012). The application of this model is limited to metal wall loss due internal or external corrosion. The corrosion defect depths are between 20 % to 80 % of the wall thickness. It is used for determination of the remaining strength of the corroded pipes and estimating of the maximum allowable operating pressure are shown in Equation (2.9) and (2.11).

$$P = \left\{ \frac{2t(1.1\sigma_y)}{D} \cdot \frac{1 - \dfrac{2d_{max}}{3t}}{1 - \dfrac{2d_{max}}{3tM_1}} \right. \tag{2.9}$$

$$\frac{d_{max}}{t} \leq 0.8 \, and \, \frac{L^2}{Dt} \leq 20$$

$$M_1 = \sqrt{1 + \frac{0.8L^2}{Dt}} \tag{2.10}$$

or

$$P_{b1} = \frac{2t(1.1\sigma_y)}{D}\left(1 - \frac{d_{max}}{t}\right) \tag{2.11}$$

$$\frac{d_{max}}{t} \leq 0.8 \, and \, \frac{L^2}{Dt} \rangle 20$$

The parameter shown above describe as maximum pressure P , pipe wall thickness t , yield strength σ_y , pipe outer diameter D, maximum depth of corrosion d_{max} , constant M_1 , and length of crack L.

2.5.3 Modified B31G

Modified B31G model was derived from ASME B31G model. The modification is occurred due to the effective corrosion area and flow stress (Belachew et al., 2009). This modification results in the change of the failure equation, which is also dependent on the limit on defect length. The equation to calculate the failure pressure is modified is shown in Equation (2.12).

$$P = \frac{2t(\sigma_y + 68.95)}{D} \frac{1 - \dfrac{0.85d_{max}}{t}}{1 - \dfrac{0.85d_{max}}{tM_2}} \quad (2.12)$$

$$\frac{d_{max}}{t} \leq 0.8$$

$$M_2 = \sqrt{1 + 0.6275\frac{L^2}{Dt} - 0.003375\frac{L^4}{(Dt)^2}} \qquad \frac{L^2}{Dt} \leq 50 \quad (2.13)$$

$$M_2 = 3.3 + 0.032\frac{L^2}{Dt} \qquad \frac{L^2}{Dt} > 50 \quad (2.14)$$

The parameter shown above describe as maximum pressure P, pipe wall thickness t, yield strength σ_y, pipe outer diameter D, maximum depth of corrosion d_{max}, constant M_2, and length of crack L.

2.5.4 DNV-RP-F101

The DNV-RP-F101 model assessment is for pipeline containing single defect, multiple interacting defects and complex shape defect as well as single defect under combined internal pressure. The defect depth for this model is not exceeding 85 % of the wall thickness (Belachew et al., 2009). The burst pressure is calculated as written in Equation (2.15).

$$P = \frac{2t\sigma_u}{D - t} \frac{1 - \dfrac{d_{max}}{t}}{1 - \dfrac{d_{max}}{tM_3}} \quad (2.15)$$

$$\frac{d_{max}}{t} \leq 0.85$$

$$M_3 = \sqrt{1 + \frac{0.31L^2}{Dt}} \quad (2.16)$$

The parameter shown above describe as maximum pressure P , pipe wall thickness t , ultimate tensile strength σ_u , pipe outer diameter D, maximum depth of corrosion d_{max} , constant M_3 , and length of crack L.

2.5.5 RSTRENG

Remaining Strength of Corroded Pipe is a modified B31G based on real shape of corrosion defects. The basic difference between the Modified B31G and RSTRENG is the geometry description. The modified B31G method can be taken as a simple calculation with an approximate geometric shape, while RSTRENG takes into account the actual profile of the defect is shown in Equation (2.17).

$$P = \min\{P_{b4}^{j}\} \quad j = 1, 2, ..., m$$

$$P^{j} = \frac{2t(\sigma_y + 68.95)}{D} \frac{1 - \dfrac{A_j}{L_j t}}{1 - \dfrac{A_j}{M_2 L_j t}} \tag{2.17}$$

$$\frac{d_{max}}{t} \le 0.8$$

$$M_2 = \sqrt{1 + 0.6275\frac{L^2}{Dt} - 0.003375\frac{L^4}{(Dt)^2}} \qquad \frac{L^2}{Dt} \le 50 \tag{2.18}$$

$$M_2 = 3.3 + 0.032\frac{L^2}{Dt} \qquad \frac{L^2}{Dt} > 50 \tag{2.19}$$

The parameter shown above describe as maximum pressure P , pipe wall thickness t , yield strength σ_y , pipe outer diameter D, maximum depth of corrosion d_{max} , constant M_2 , and length of crack L.

2.5.6 PCORCC

PCORRC equation proved to be conservative and the closest when using 95 % of UTS of tensile test, $\sigma_{U,Test}$ as σ_U. The C value varies from 0.142 to 0.224 with the change of pit depth (Belachew et al., 2009). However for conservative prediction of damaged pipe, the maximum value is 0.224 as curve fit constant and the above equation is written as Equation (2.20).

$$P = \frac{2\sigma_u t}{D}\left[1 - \frac{d_{max}}{t}\left(1 - \exp\left(\frac{-C L}{\sqrt{\frac{D(t - d_{max})}{2}}}\right)\right)\right] \quad (2.20)$$

$$L \leq 2D \, and \, \frac{d_{max}}{t} \leq 0.8$$

The parameter shown above describe as maximum pressure P, pipe wall thickness t, ultimate tensile strength σ_u, pipe outer diameter D, maximum depth of corrosion d_{max}, and length of crack L.

2.6 CAUSE OF PIPELINE FAILURE

2.6.1 Introduction

Failure of a natural gas transmission service is extremely serious because it can give potential for loss of life. Cracks may develop in pipelines at any time due to its surrounding condition. During pipeline operation, existing defects may grow due to fatigue. Moreover, crack growth mechanism includes external stress corrosion cracking (SCC), stress-oriented hydrogen induced cracking (SOHIC) and hydrogen induced cracking (HIC) are the several factors that contribute to the failure of pipeline.

2.6.2 Stress Corrosion Cracking (SCC)

The stress corrosion cracking is cause by the exposure of the pipe external surface to the wet soil around it. This normally happen to the buried pipeline as the pressure and the temperature of pipe working condition is lower than the allowable limits. As the result of the chemical interactions and formation of carbonate or bicarbonate solution and with the presence of tensile stresses, stress corrosion cracking occurred in longitudinal direction and at the outer surface of the pipeline (Kim et al., 2008). The natural soil environment that contains several amount of moisture and oxygen combine with the stress such hoop stress and residual stress cause the initiation of cracking in the pipe thickness. Formation of carbonate or bicarbonate is related to the presence of environment with the high pH value at the cracked region where the pH value was between 8 and 10 (Kim et al., 2008).

SCC risk can be minimized on new pipelines by careful coating selection and preservation of coating condition through the construction process. To reduce SCC risk, priority should be placed on the long-term adhesion performance of the coating and its resistance to adhesion loss from water uptake, cathodic disbonding, soil induced loading and impact or gouging.

2.6.3 Stress-Oriented Hydrogen Induced Cracking (SOHIC)

A special form of HIC may occur when local stress concentration is very high in a sour service pipeline. High stress fields allow the hydrogen to accumulate without the need for inclusions or other interfaces. For example, some types of spiral-welded pipe exhibit highly stressed regions close to the seam weld, caused during the edge forming process. Stacked arrays of HIC can form in these regions, leading to rapid stepwise cracking failures (Kim et al., 2008).

2.6.4 Hydrogen Induced Cracking (HIC)

Sour service pipelines are vulnerable to HIC in the presence of water. It can occur in pipeline steels of any strength and is generally associated with nonmetallic inclusions, particularly elongated manganese sulfides. Features within the pipe wall appear as cracks, but features near the surface appear as blisters or bumps. Acid corrosion takes place on water-wetted areas inside the pipeline. Hydrogen is produced by this corrosion reaction, but in the presence of sulfide, scales on the steel surface rather than being liberated as a gas. The atomic hydrogen diffuses into the steel, forming blisters in the microscopic voids around non-metallic inclusions. HIC develops as flat cracks in the rolling plane of the pipe material. Crack colonies develop, and failure often occurs as colonies link together in a stepwise fashion and for this reason, HIC is sometimes called stepwise cracking (Kim et al,. 2008).

2.7 CHEMICAL COMPOSITION

Table 2.2 shows the chemical composition of standard API 5L X42, X52 and X60 steel pipe. Table 2.3 shows the chemical composition of material Grade B from spectro-analysis that used in the simulation.

Table 2.2: Chemical composition of API 5L X42, X52 and X60 steel.

Type of API steel pipe	Element (%)				
	C	P	Mn	S	Si
API 5L X 42	0.24	0.25	1.2	0.015	0.40
API 5L X 52	0.24	0.25	1.4	0.015	0.45
API 5L X 60	0.24	0.25	1.7	0.015	0.45

Source: ANSI/API Specification 5L (2007)

Table 2.3: Chemical composition of material Grade B.

Material Grade B	C	P	Mn	S	Si
	0.258	0.01	0.559	0.001	0.309

2.8 FAILURE CRITERION

2.8.1 Maximum Shear Stress

Maximum shear stress theory often refers as Tresca theory. This theory used for predicting the failure of material due to maximum shear stress applies in material is exceeds the yield shear stress. Yield in ductile materials is usually caused by the slippage of crystal planes along the maximum shear stress surface and there is certain point in the body is considered safe as long as the maximum shear stress at that point is under the yield shear stress τ_y obtained from a uniaxial tensile test as shown in Figure 2.2 (Efunda, 2012).
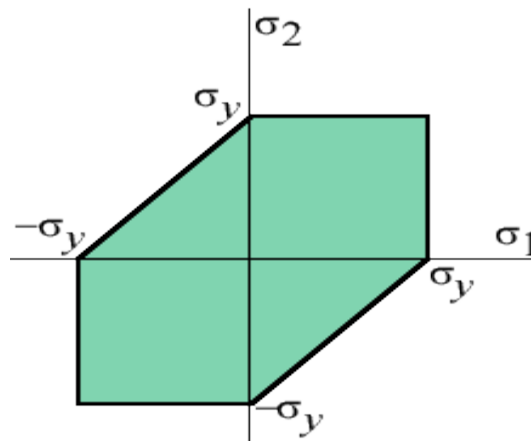
Figure 2.2: Maximum shear stress.

Source: www.efunda.com

If $\sigma_1, \sigma_2, \sigma_3$ are the three principal normal stresses from applied loading, then from Mohr circle, the maximum shear stress in the part is,

$$\tau_{max} = [\sigma_1 - \sigma_2/2, \sigma_2 - \sigma_3/2, \sigma_1 - \sigma_3/2]$$
(2.21)

In uniaxial testing, the tensile stress was σ_y during yielding. In this case, $\sigma_1 = \sigma_y, \sigma_2 = \sigma_3 = 0$. Thus, again from Mohr circle, shear stress $\tau_y = \sigma_y/2$. Failure will occur when

$$\tau_y = \tau_{max} \text{ or } [\sigma_1 - \sigma_2/2, \sigma_2 - \sigma_3/2, \sigma_1 - \sigma_3/2] = \sigma_y/2$$
(2.22)

2.8.2 Von Mises Stress

The maximum distortion energy theory is also known as the von Mises theory. In this theory, failure will occur when the distortion energy per unit volume due to the applied stresses in a part equals the distortion energy per unit volume at the yield point in uniaxial testing.

The von Mises theory is used for ductile materials and is seen most often when evaluating stresses, both static and dynamic, for shafts. In an elastic body that is subject to a system of loads in 3D, a complex 3D system of stresses is developed. That is, at any point within the body there are stresses acting in different directions, and the direction and magnitude of stresses changes from point to point. The von Mises criterion is a formula for calculating failure by yielding. The equivalent stress in general form is then given by (Budynas and Nisbett, 2011).

$$\sigma_{vm} = \sqrt{\left[\frac{(\sigma_1 - \sigma_2)^2 + (\sigma_2 - \sigma_3)^2 + (\sigma_1 - \sigma_3)^2}{2}\right]}$$
(2.23)

as for plane stress case $\sigma_3 = 0$. Then the von Mises criterion reduce to

$$\sigma_{vm} = \sqrt{\sigma_1^2 - \sigma_1\sigma_2 - \sigma_2^2}$$

(2.24)

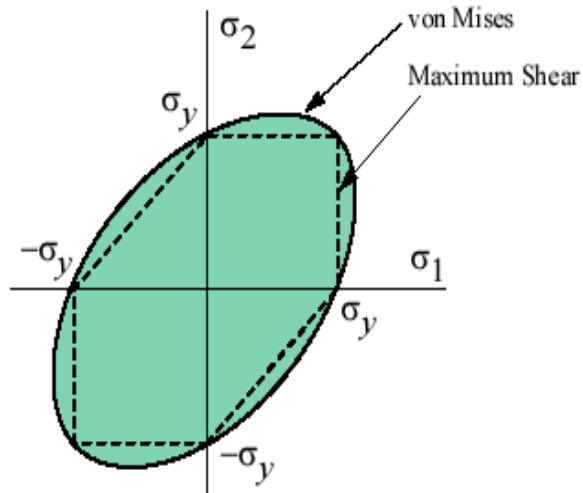This equation represents a principal stress ellipse as illustrated in the following Figure 2.3.

Figure 2.3: Tresca and von Mises plane surface.

Source: www.efunda.com

CHAPTER 3

METHODOLOGY

3.1 INTRODUCTION

This chapter will describe about the procedures used to carry out this project during the analysis work on the defects in the pipeline from the beginning until complete simulation. Methodology is needed to ensure the project can be conducted properly and smoothly then produce better results based on objectives. The process flow chart is used to make the work easier to monitor as it shows step by step taken in this project. The arrangement of the steps provides the report become more structured and easy to understand.

3.2 METHODOLOGY FLOW CHART

There are a few steps taken such creating the geometries, meshing the elements, applying loads and boundary condition, selecting material properties, run the simulation and analysing results should be concerned during the simulation. All the steps needed must follow the sequence to avoid any mistake and error at the end of the analysis. The procedure for this analysis is starting from modeling the design geometry until analysed the result is shown in Figure 3.1.
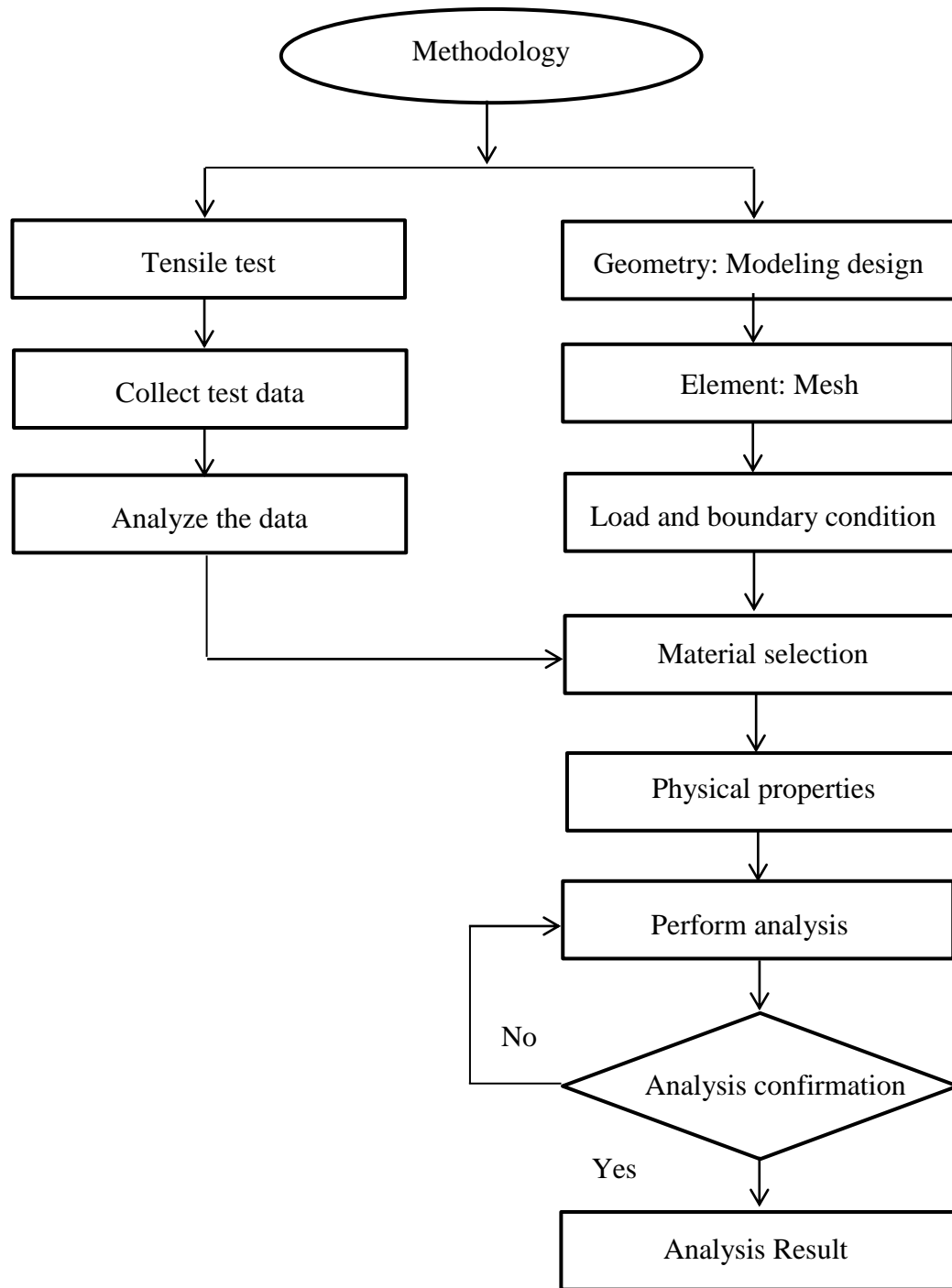
Figure 3.1: Methodology flow chart.

3.3 MECHANICAL PROPERTIES

Tensile test data is collected from the available data base on the tensile test of specimen material in order to find the mechanical properties. The specimen was machined according to ASTM E8 2008 specification for plane tensile test specimen. ASTM E8 is the specification for the test methods that cover the tension testing of metallic materials in any form at room temperature, and more specifically, the methods used to determine yield strength, yield point, tensile strength, elongation, and reduction of area. The data from the test were analysed and converted into engineering stress strain graph and then into a true stress strain for the use of the simulation process. The true stress strain curve was adopted from tensile test result which was performing from the same material as the burst pressure specimen.

3.3.1 Engineering Stress Strain

Initially, the tensile tests are performing to find the mechanical properties of the material that used for the experiment. The basic data used to know the mechanical properties are obtained from this test. The data obtained from this test including ultimate tensile test, yield strength, strength at break and maximum load.
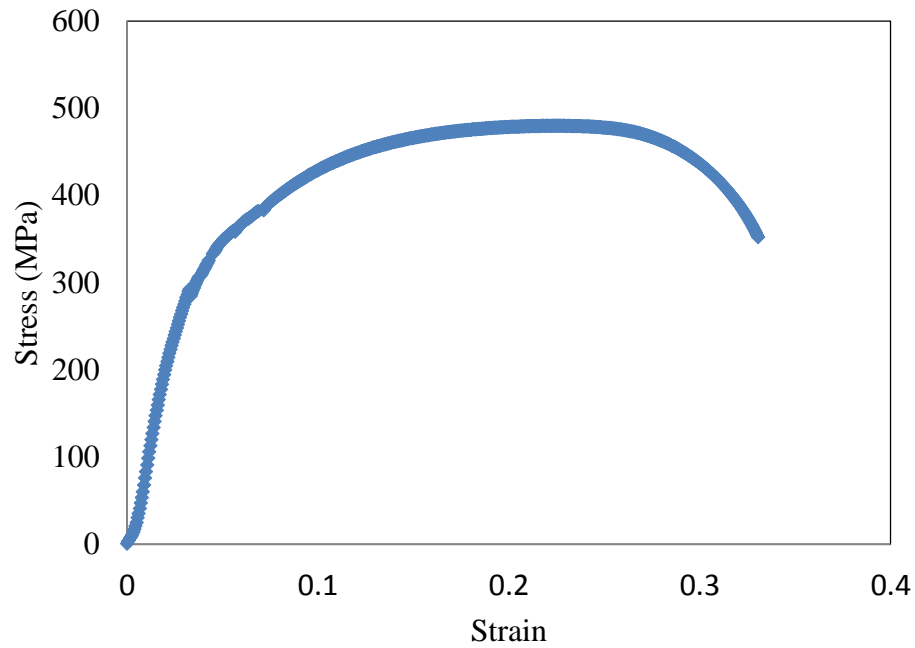
Figure 3.2: Engineering stress strain curve of Material Grade B.

Table 3.1: Mechanical properties of Material Grade B obtained from tensile test.

Yield strength (MPa)	326
Ultimate tensile strength (MPa)	465
Elastic modulus (MPa)	207 000
Poisson ratio	0.3

3.3.2 True Stress Strain

In finite element analysis (FEA), true plastic stress-strain data must be employed as an input data for the material. Therefore, it is very important to convert engineering stress- strain data into true stress-strain data. There are the steps to convert the data which is by using the equations and the equation are given by:

$$\sigma_t = \sigma_e(\varepsilon_e + 1) \tag{3.1}$$

$$\varepsilon_t = \ln(1 + \varepsilon_e) \tag{3.2}$$

The Equation (3.1) and (3.2) are only applicable up to necking point of the material and Figure 3.3 shows the it can be concluded that the stress is increasing after the maximum point up to fracture. This is because due to the reduction of cross-section area of the material after necking was occurring. The true stress-strain data from necking point to fracture was predicted based on a power law equation that is given by:
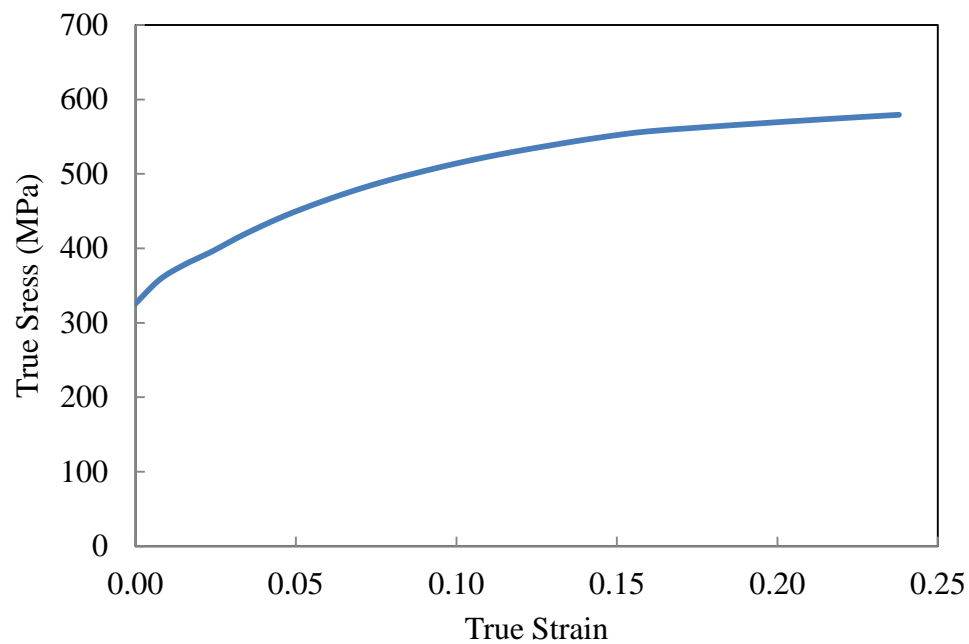
$$\sigma_t = k\varepsilon^n \tag{3.3}$$

Figure 3.3: True plastic stress strain curve of Material Grade B.

Based on the true plastic stress-strain curve shown in Figure 3.3, it can be concluded that the stress is increasing after the maximum point up to fracture. This is because due to the reduction of cross-section area of the material after necking was occurring. Besides that, the pattern of this graph of stress-strain for Material Grade B was affected by the value of strain hardening coefficient and strain hardening exponent.

3.4 FINITE ELEMENT ANALYSIS (FEA)

For the analysis work, finite element method (FEM) is used. This project uses finite element analysis software called MSC Patran 2008 r1 for pre-processing and post-processing. Besides, MSC Marc 2008 r1 is used as a solver in this project. The steps and explanations on how each procedure is taken are described further to make sure the procedure is correct. The steps are arranged properly for better understanding and easier to follow.

3.4.1 Modeling Design

The model was designed using MSC Patran 2008 r1. Firstly, the preferences and analysis code were set to MSC Marc as shown in Figure 3.4 (a). Geometry scale factor then was changed into the millimeter and the modeling process was started. Figure 3.5 shows the icon bar for each step taken to do the simulation.
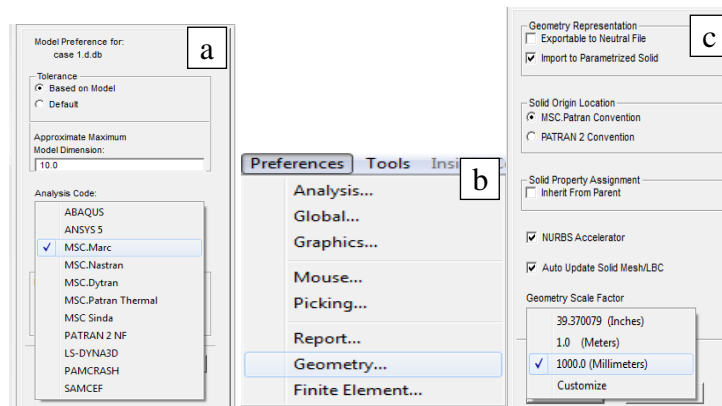
Figure 3.4: Initial steps using MSC Marc: a) MSC Marc code, b) Geometry from Preferences, and c) Geometry scale factor.
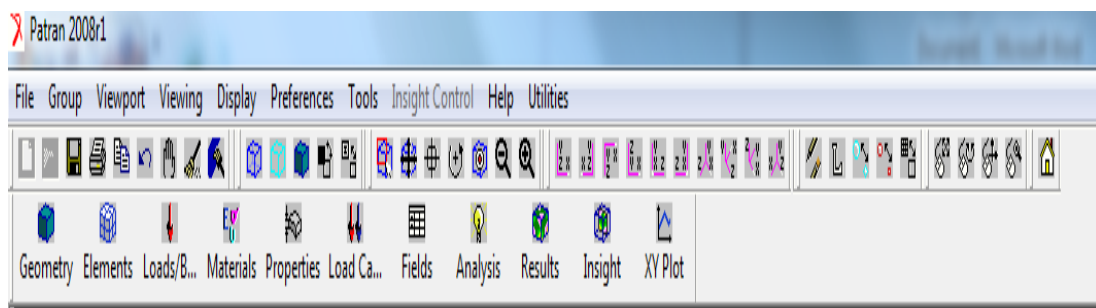

Figure 3.5: Step in PATRAN software.

During modeling design, half of the pipe is created for the simulation and analysis due to the symmetrical shape of the defect in the pipe. The model of the half pipe with the outer diameter, OD 60.5 mm, 4 mm thickness of pipe, t and 600 mm long, L were constructed to analyse the defect. There are 16 cases of multiple types of defects that formed from two cracks with various crack distance. Two identical cracks were created between a distance with collinear aligned to identify the interaction during the analysis. The first crack length is same as the second crack length which represent by 2c. The parameters such crack distance, d are varied while the width and depth of the crack are same for each model which is 0.2 mm and 2 mm respectively. All the dimensions are

from the small scale test are shown in Table 3.2 and the defect designs are described as in Figure 3.6.

Table 3.2: The defect size.

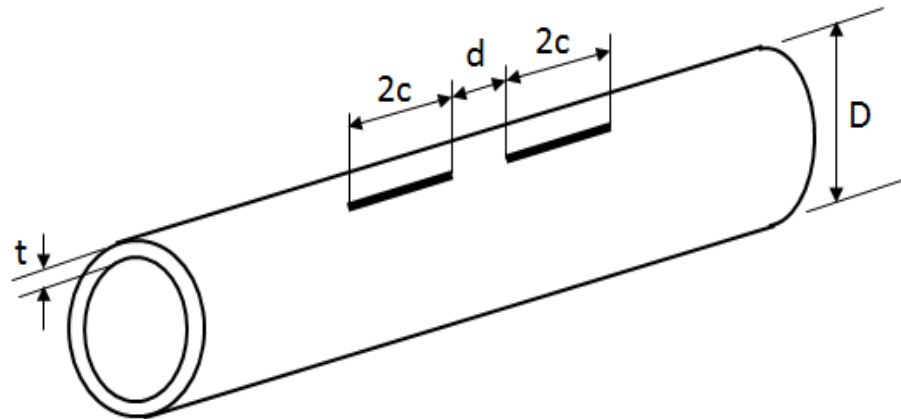| Defect configuration	Defect size 2c (mm)	Distance between cracks d (mm)
Case 1	25	0.5
Case 2		2
Case 3		4
Case 4		8
Case 5	50	0.5
Case 6		2
Case 7		4
Case 8		8
Case 9	75	0.5
Case 10		2
Case 11		4
Case 12		8
Case 13	100	0.5
Case 14		2
Case 15		4
Case 16		8

Figure 3.6: Pipe with two collinear defects.

The pipe has been drawn in 3D (three dimensions) by using coordinate to obtain the shape of pipe in half. In order to create the point, all point coordinate must need to know. To start the drawing, the coordinate of the point was inserted in the Point Coordinate List column. Finish plot all points by entering the coordinates then proceed to create the curve are shown in Figure 3.7 (a). Figure 3.7 (b) shows how to make a straight that connect between two points by selecting Create then Curve. Then first point was selected as the starting point and it will show in the Starting Point List and picked the second point as the end point and it will show in Ending Point List. Curve line can be made by selecting method 2D Arc2Point is shown in Figure 3.7 (c).
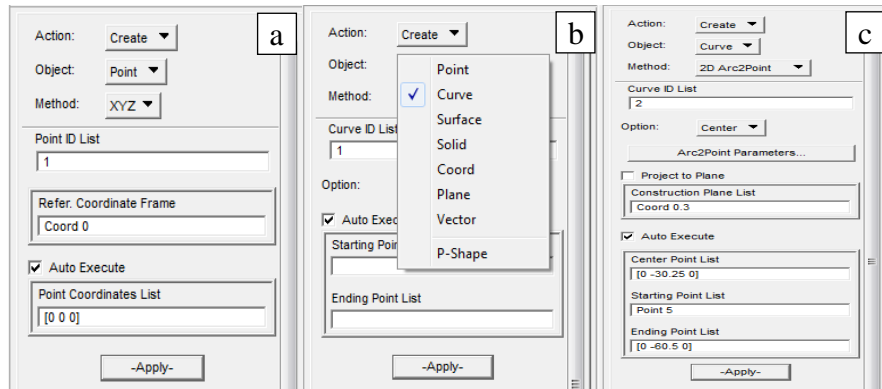
Figure 3.7: Step in making line: a) Create point, b) Create straight line, and c) Create curve line.

At the inside crack edge, small fillet is made by selecting Fillet method and put the value of radius for the fillet in the Fillet Radius column. Then two lines that are connected by the fillet were selected are shown in Figure 3.8 (b).
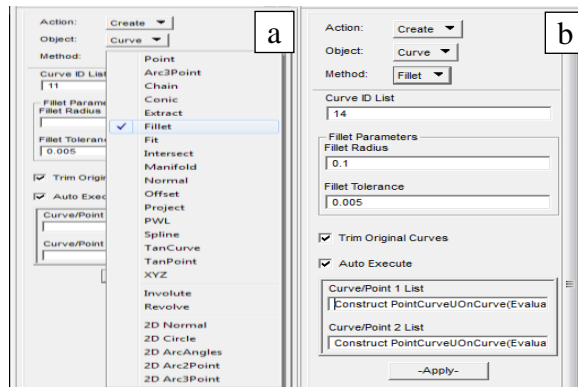

Figure 3.8: Step for fillet: a) Create fillet, and b) Insert the radius and curve list.

Figure 3.9 (a) show the point and the line that have been construct at the crack part and Figure 3.9 (b) show the total drawing of the half pipe. Both figures are created in x and y axis. Then select Surface to create surfaces for the drawing is shown in Figure 3.10 (a). Surface can be created by selecting the Starting and Ending Curve List. Figure 3.10 (b) shows four surfaces that have been created.
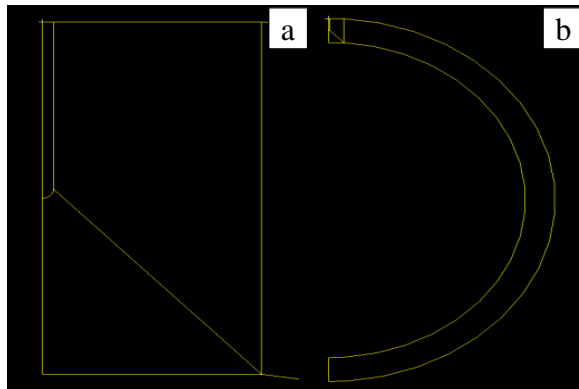
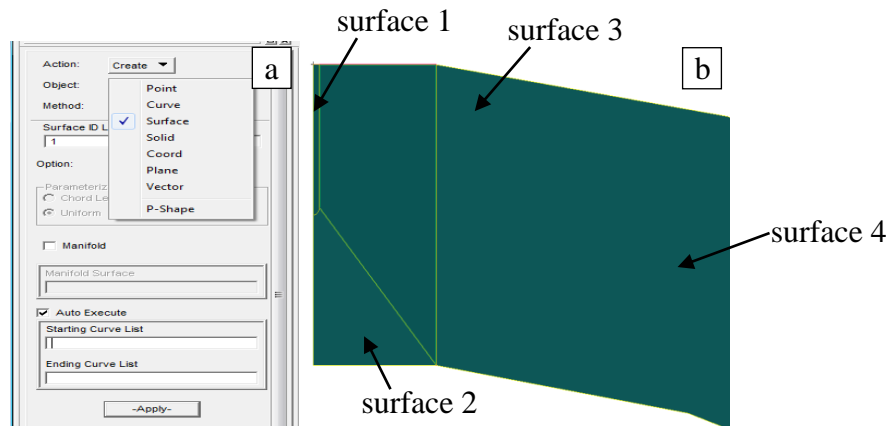**Figure 3.9:** 2D drawing: a) Fillet, and b) Curve.

Figure 3.10: Step for surface: a) Create surface, and b) Surface selection.

To make the 3D model, all the surfaces need to be extruded. Select Solid then follows by choosing Extrude method. The direction of the extrusion is in the z axis direction, and then a value was entered in the Translation Vector column as shown in Figure 3.11 (c). Figure 3.9 shows the step to create a solid using extrude method.
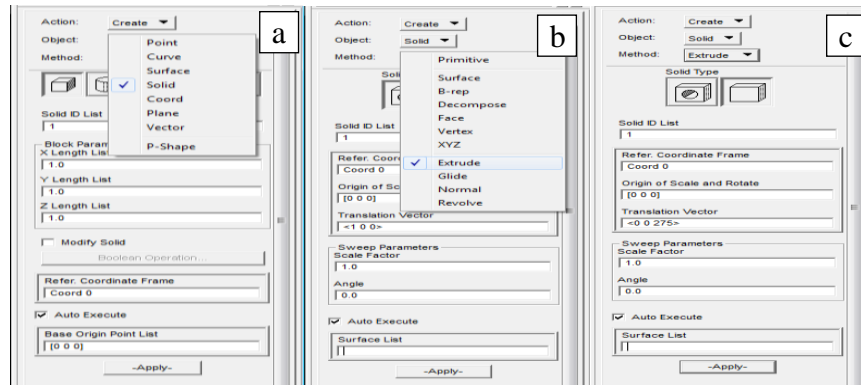
Figure 3.11: Step for solid extrude: a) Create solid, b) Extrude, and c) Input Translation vector.

To make an empty space as the crack part, the crack surface should be transform. The selected surfaces transform 25 mm in z axis direction. Figure 3.12 (a) show how to transform the crack surface and Figure 3.12 (b) the surface that has been transform.
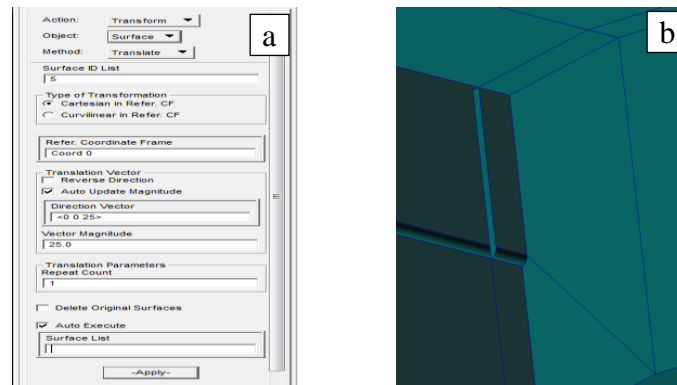

Figure 3.12: Step using surface transform: a) Select surface transform, and b) Transformed surface.

The pipe model has now been half way finished. The model then continuously extrudes using the same method until reaches the other end of the pipe.

3.4.2 Create Element

After that, the Element part for the model was created by using mesh. Figure 3.13 show the first step in Element part that is the mesh seed process for the model. In this project, two types of mesh seed are used to get the suitable meshes that are uniform mesh and one way bias mesh.
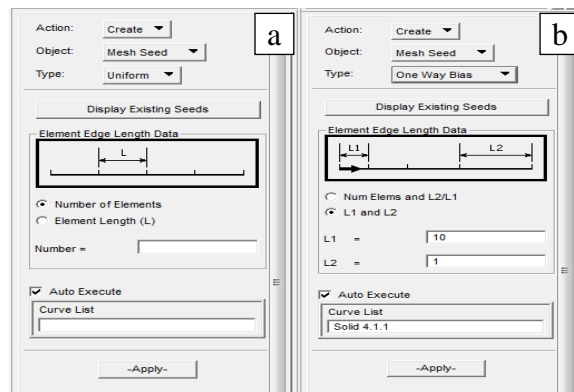

Figure 3.13: Type of mesh seed: a) Uniform mesh seed, and b) One way bias mesh seed.

Mesh seed is constructed by selecting the edge of the solid model. Mesh seed is important to control the number of the element that desire. The uniform mesh seed is used to make the mesh seed located equally from each other on the same edge. One-way bias is to concentrate at the end of the edge while two-way bias is to concentrate at both of the end of the edge. The number of the mesh seed can be controlled by manual input. Mesh seed and global edge length are the two ways for controlling the element size. After that, create the mesh using Mesh geometry to generate mesh and select Solid to mesh the entire solid body of the model. This meshing is done by using Automatic Global Edge Length. From these meshing, the fine and coarse mesh can be produced. Use the Hex element shape and select Solid to be meshed in a Solid List column. When creating the New Property, use 3D solid and set the property name as 'steel'. Make sure Standard Geometry and Reduce Integration is chosen before input the properties. Figure

3.14 (a) and (b) show the meshing step of the solid model of the pipe. After that, all the meshing has been equivalence to connect the mesh in the solid part of the model as shown in Figure 3.14 (c). Equivalence is the process of reducing all nodes that coexist at a point to a single node. Equivalence under these circumstances will remove duplicate nodes which match from both sides. This will leave all other nodes which do not coincide. The mesh is now continuous and without cracks and the redundant nodes have been deleted.
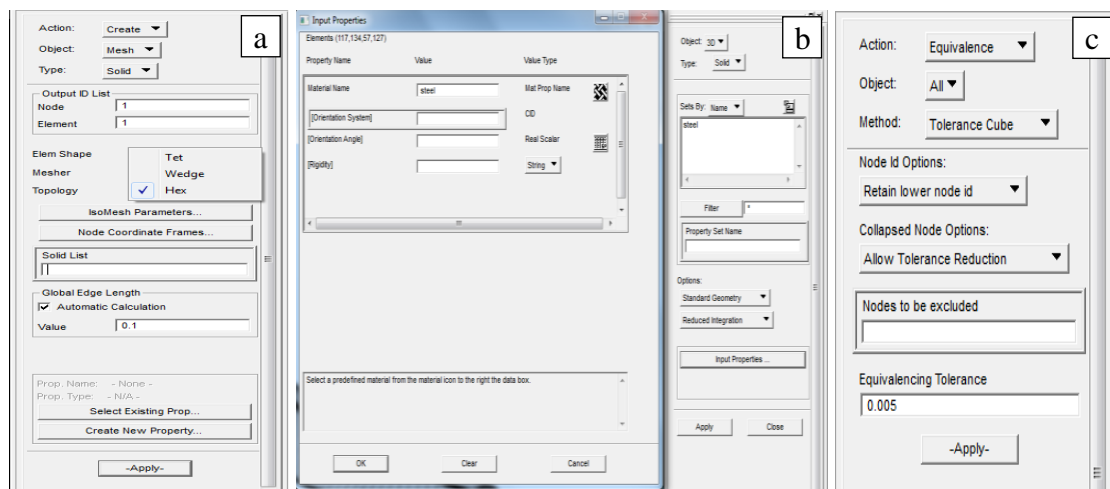

Figure 3.14: Step for meshing: a) Select Element Shape, b) Input material properties, and c) Equivalence.

Figure 3.15 (a) show the pipe model that has been completely mesh while Figure 3.15 (b) is the meshing at the distance between crack parts. The sizes of the mesh are quite small between the crack compare at the other part of the pipe model. It shows that the interest region being concerned in the simulation. Furthermore, the number of the mesh can increase the accuracy of the simulation result.
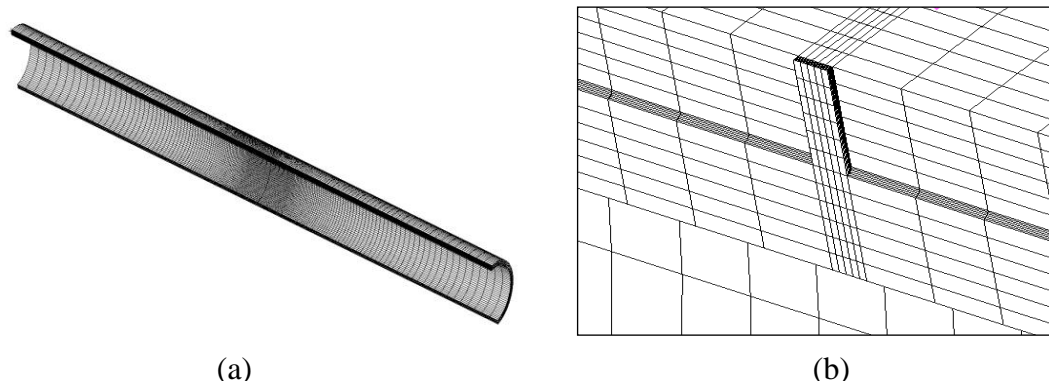
Figure 3.15: Complete mesh: a) Mesh model, and b) Mesh at defect of pipe.

3.4.3 Loads/ Boundary Condition

The Loads and Boundary Conditions application (Loads/BCs) provides the ability to apply a variety of static or dynamic loads and boundary conditions to finite element models. Loads/BCs may be associated with geometric entities as well as FEM entities. When associated with geometric entities, they can be transferred to finite elements created in the geometry. To create a new load, a new name for every load that's needed was set. For example, to set the boundary condition for both surfaces at the ends of the model, select Displacement as shown in Figure 3.16 (a). Fixed was written as a name for the boundary condition that need to be created. Then click on Input Data option and enter the translational and rotational value. After that, click on Select Application Region to choose and put the boundary in the model. For the fixed both ends of the model the translational value is <0,0,0> while the rotational is <0,0,0>. For the surface of the model which is symmetry to the x axis, the translational value is <0, , > while the rotational is < ,0,0>. The steps for the fixed boundary condition show in Figure 3.16.
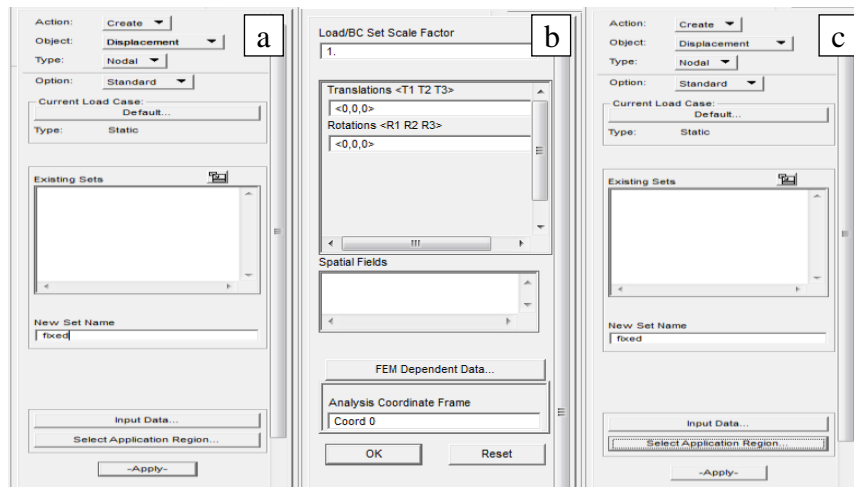
Figure 3.16: Step for boundary condition: a) Fixed boundary, b) Input fixed condition, and c) Select surface.

Next, the internal pressure is applied to the inner surface of the pipe model. The Displacement was change into Pressure and gives a name for the pressures apply. Then click on Input Data to key in the pressure value in the Pressure column. After that, click on Select Application Region for selecting all inner surfaces of the pipe model that surrounded the pressure. Figure 3.17 shows the step to set the pressure applied.
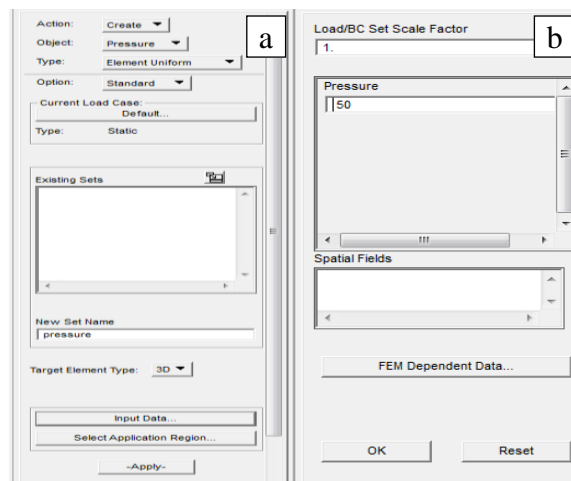

Figure 3.17: Pressure setting step: a) The pressure name. b) Input pressure value.

3.4.4 Field

The fields are used to define loads and boundary conditions as a function of one, two, or three variables; material properties as functions of temperature, strain, strain rate, time and frequency. Data Fields are used in the material properties, loads and boundary conditions, and element properties applications. Fields can be either scalar or vector in nature. An important purpose of the Fields functionality is to provide a means of interpolating, or applying the results of one finite element analysis onto the same or different geometry or FEM model. Real scalar, complex scalar, and real vector results can be interpolated.

To create a new field, Patran Fields application button was selected to display the fields form. The Create action was selected, followed by the Object to be created that is Material Property. Before continuing, a choice can be made between creating all new fields, and creating one like an existing field. Upon selection of the object, Patran will display any existing fields of the same object type in the Existing Fields box. Then, enter any field name, click on strain and select Input Data to export the CSV file of the data are shown in Figure 3.18.
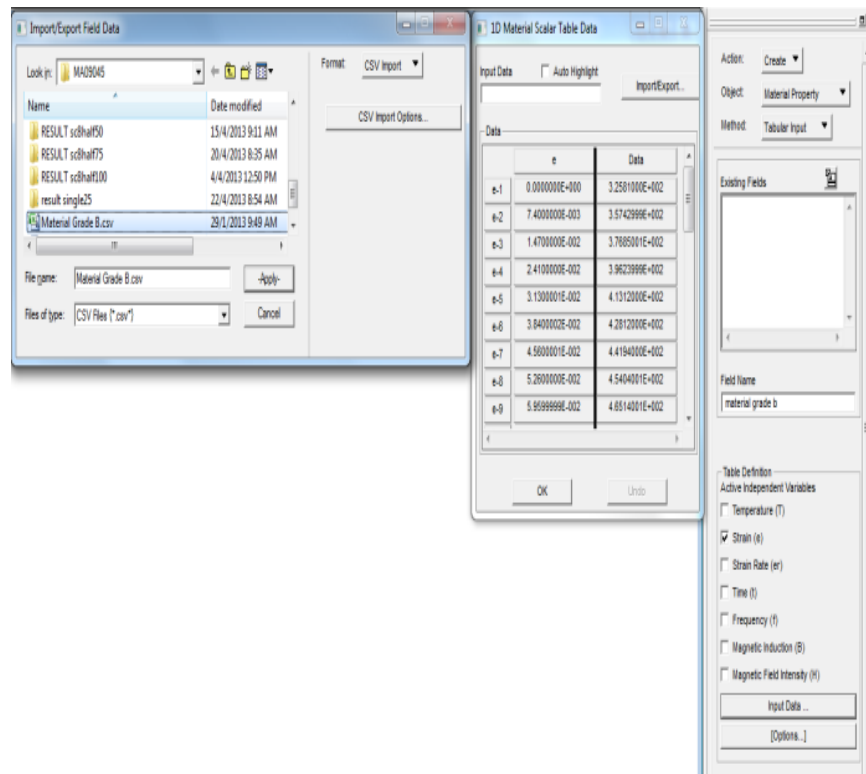
Figure 3.18: Input the field properties.

As engineers are often supplied with engineering stress and strain test data, a conversion to true stress and strain is needed before inputting these material properties into data fields. Engineering stress and strain test data was getting from experiment. To get the true stress and strain, engineering stress and strain can be converted to true stress by using Equation (3.1) and (3.2).

3.4.5 Material

The next step is selecting the Material part and name the material. Click Input Properties to put all the data for elastic and plastic region. There are two important data must be obtained in this part. Firstly is elastic region data that need to fill are young modulus and poisons ratio of the material used. The value of young modulus and poisons ratio for each material are stated in Table 3.1. Secondly is plastic region data

that need to take from the Field part is true plastic stress-strain data for the material need to run shown in Figure 3.19.
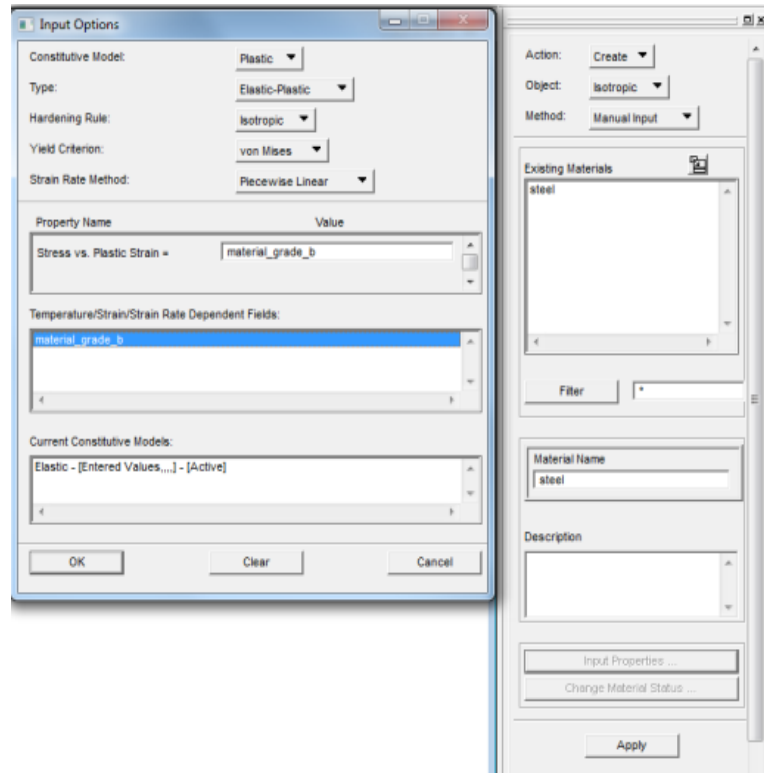

Figure 3.19: Plastic model option.

3.4.6 Properties

After that, the Properties part has been done to ensure the finite element analysis Patran 2008r1 software can read the properties given and run the simulation successful. The object part was changed to become 3D in order to ensure the software read the specimen in 3D. Then, the property name is given. After that, Option is clicked and Reduce Integration is chosen for this part. For Input Properties, the box that shown in Figure 3.20 should be clicked and then took the data needed. Lastly, the Application Region was chosen to apply for all the properties selected.
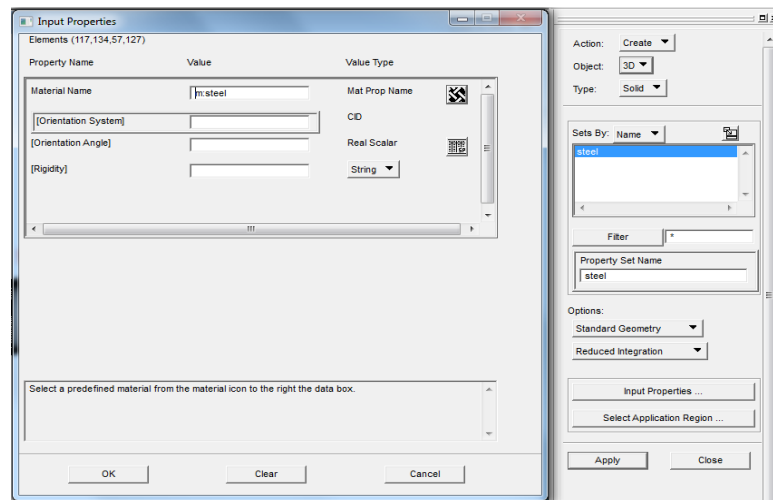
Figure 3.20: Set the material name.

3.4.7 Analysis

Next is the Analysis part. In this part all the parameters for analysis will be set up before run the analysis. The method must be changed into Analysis Deck and a name is given to the job. The name to be attached to all files associated with this particular run should be defined first before create a new job. Every analysis job name must be unique for a particular analysis code. The same job name must be used for both the Analysis and the Read Results File selections if the results are to be loaded into the originating load cases. These analysis job names are stored in the database and are used to correlate the load cases selected in analyse with the load cases it is found in Read Results File.

After that, Job Parameter is clicked and the data needed is filled. Then clicked on Solver to get same as Figure 3.21 and followed by Non-Positive Definite. For further analysis, Load Step Creation is selected and then the Load Step Name is changed. After that, clicked on Solution Parameter and Follower Forces is checked. Then, Load Increment Parameter is selected and entered 50 for the step of the output. Iteration Parameter was selected and the value of Relative Residual Force was change to 0.001 is shown in Figure 3.22. Reducing this number will increase the accuracy of the result.

Then OK button was clicked for the entire event. Lastly, run the analysis using the CMD command to get the result of this project. The analysis is running in a command window by typing "*run_marc −j filename.dat −b n*" as a command to run the analysis.
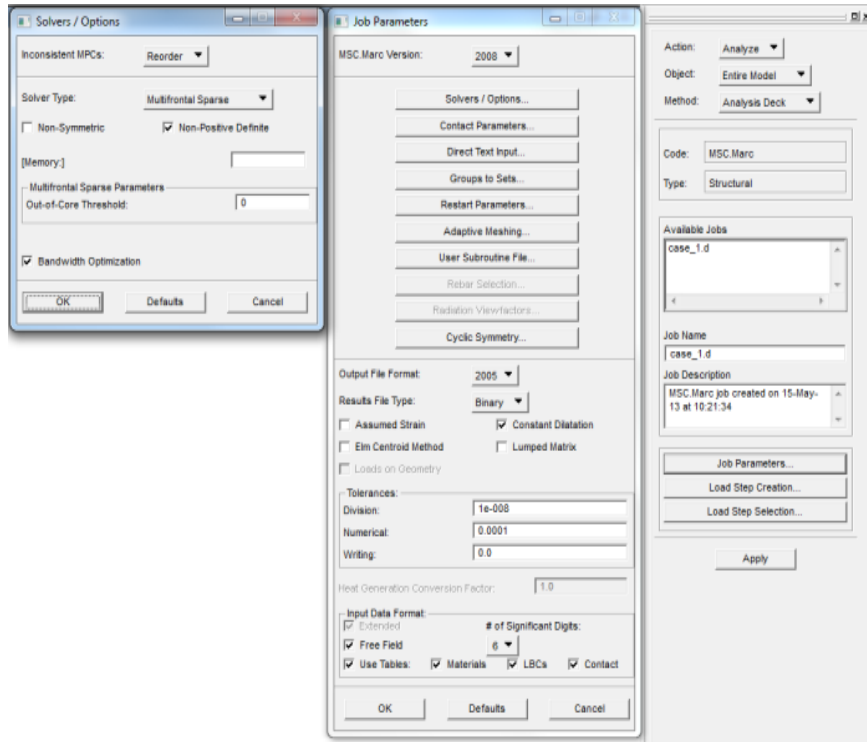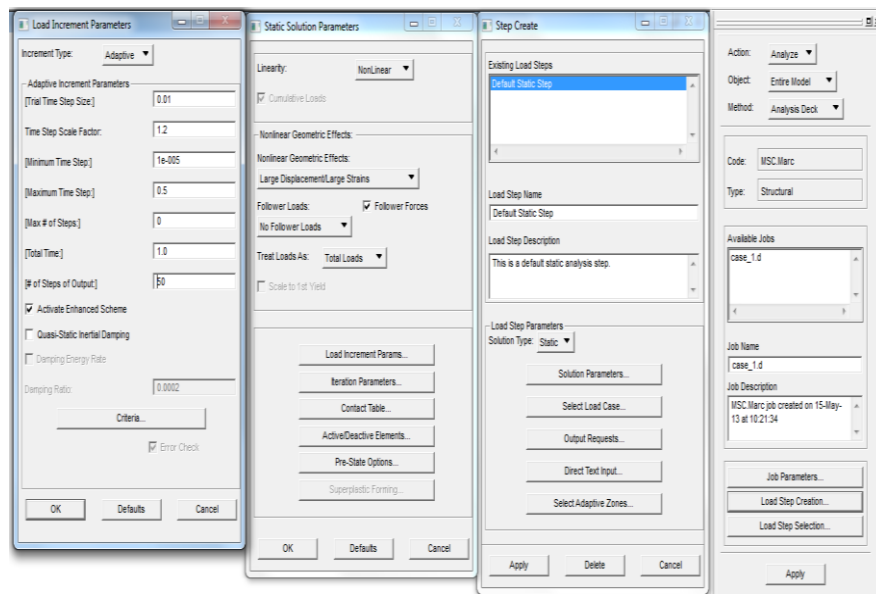

Figure 3.21: Job parameter.

Figure 3.22: Load step creation.

3.4.8 Result

The last process for Patran 2008r1 software is selecting the Result to read and analyse the result after the simulation is completely successful. Firstly, Read Result was selected then the Result File is chosen in the Analysis part is shown in Figure 3.23. Next, at Result icon the Quick Plot was selected. All Result cases are chosen and Stress Global System was select for Fringe Result. In the deformation result, Displacement, translation was chosen and the Apply button was clicked. Then the result will appear.
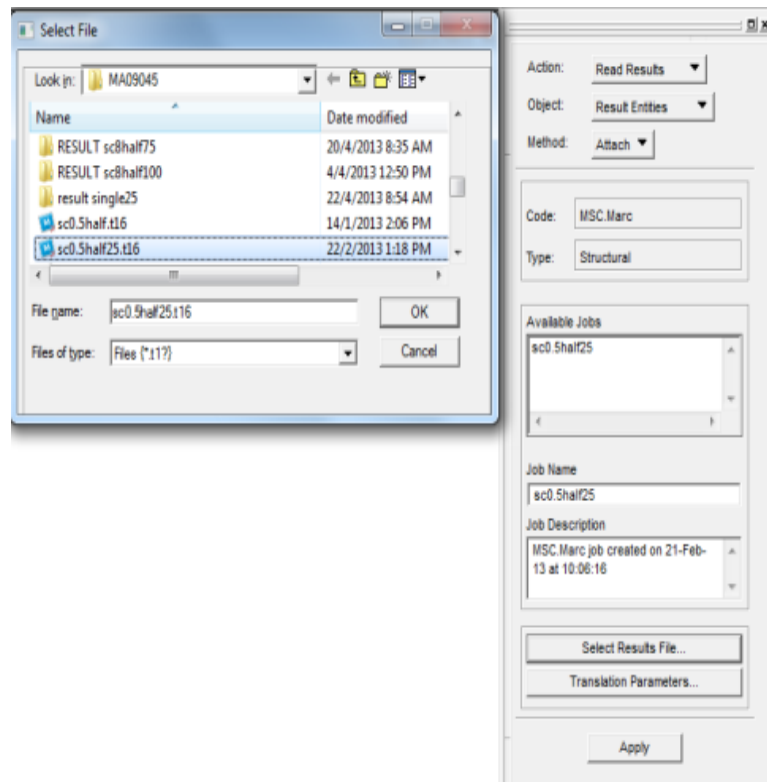
Figure 3.23: Select result file.

CHAPTER 4

RESULT AND DISCUSSION

4.1 INTRODUCTION

This chapter will discuss about the result obtain from the analysis of interaction distance between two cracks of steel pipe using finite element analysis. The objective of this project is to study the interaction of the distance between two cracks and analysing the maximum pressure for various crack distances. The result will discuss for each type of the crack distance and the failure pressure in the analysis.

4.2 RESULT AND DISCUSSUION

4.2.1 Stress Distribution along the Distance between Cracks

One of the main objectives of this analysis is to analyse the interaction of the distances between cracks. Each case of the simulation was describe in Table 3.2 as the distance between crack are varied such 0.5 mm, 2 mm, 4 mm, and 8 mm. Case 1 until Case 4 are for crack length 25 mm, while Case 5 until Case 8 are for crack length 50 mm. For the 75 mm crack length the case start from Case 9 until Case 12 and for the 100 mm crack length the Case are from Case 13 until Case 16. The maximum stress for various cracks distances and the failure pressure in the region where the cracks interact was analysed. Normally the maximum stress occurs at both ends of the distance between cracks and then it was reduced as it moves towards the centre between the cracks.

Figure 4.1 show the distribution of von Mises stress for different pressure on the distance between cracks for Case 13. The length of the crack for both left and right is 100 mm while the distance between the cracks is 0.5 mm. For pressure at 26.6 MPa the stress is higher at both ends of the distance between the cracks that is at 0 mm and 0.5 mm while the stress are slowly decrease as they approach the centre of the distance between the cracks. At this pressure level, the von Mises stress at the centre of the distance between cracks is 453 MPa. Although the stresses at both ends of the distance between the cracks are already reached the ultimate tensile strength, the defect pipe are considered not to fail yet due to the some stresses in the centre are still below ultimate tensile strength. When the pressure is increased at 27.3 MPa, Figure 4.1 shows the stress at the centre point in between the crack distance have already reached the ultimate tensile strength of the material where at this pressure the pipe was predicted to burst. Not only stress at the centre, but the stresses along the distance between cracks are also higher than ultimate tensile strength. When the pressure rises at 32.9 MPa the von Mises stress are all being equal to 579 MPa. The maximum pressure for this defect is 27.3 MPa as they reach the ultimate tensile stress.
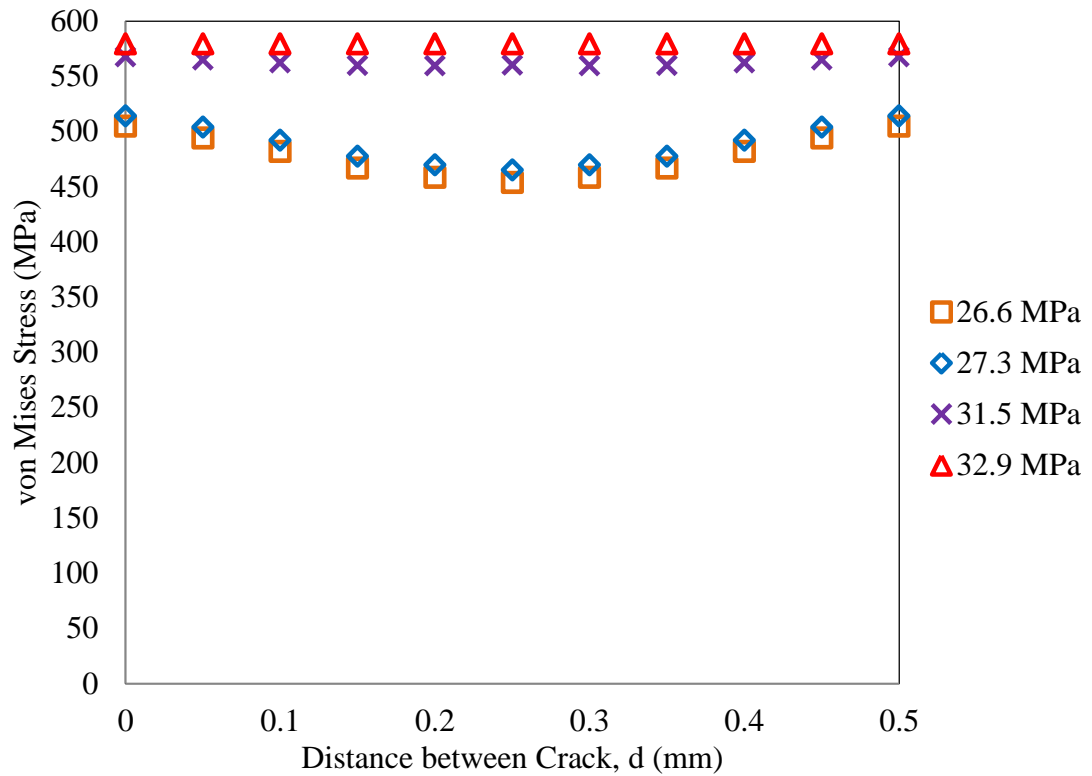
Figure 4.1: Graph Von Mises stress versus distance between cracks for Case 13.

The stress distribution for Case 13 can be seen in Figure 4.2 until Figure 4.7. The different colour shows the different von Mises stress. The red colour means the highest von Mises stress whereas the white colour represent the lowest stress. Figure 4.2 below show the zero stress at the distance between cracks as no pressure apply to the pipe model. Figure 4.3 show the stress distribution at the distance between cracks start to interact. The changes from blue to green colour show the small increment in the stress distribution. Figure 4.4 and Figure 4.5 show the stress change from green to yellow then change to purple. The purple colour region is spread at the tip of the crack and covered the region between the cracks. Figure 4.6 show the highest stress start to occur at both ends of the cracks where red colour region can be seen while Figure 4.7 show the region where the distance between cracks are completely red. At this point the stress reaches the maximum value which is 579 MPa.
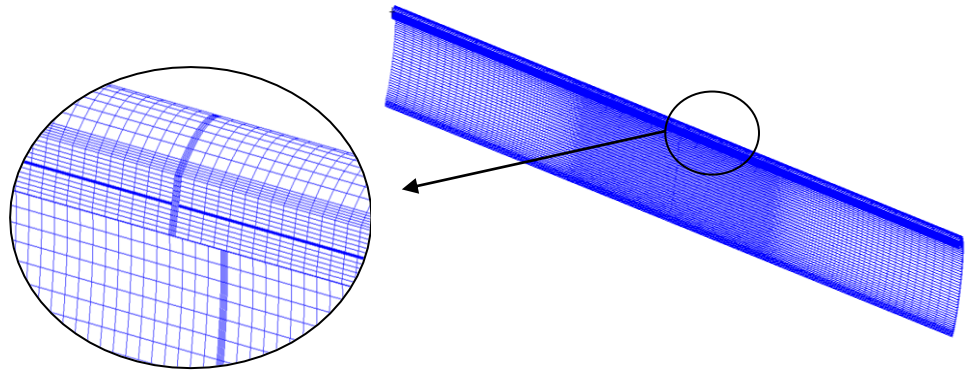
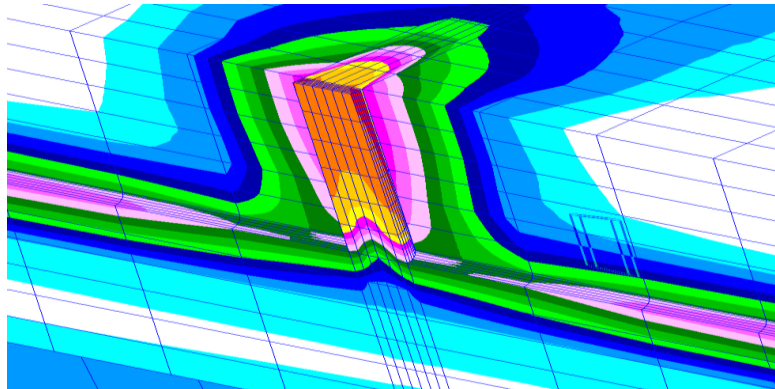**Figure 4.2:** Stress distribution at pressure 0 MPa.

Figure 4.3: Stress distribution at pressure 10 MPa.
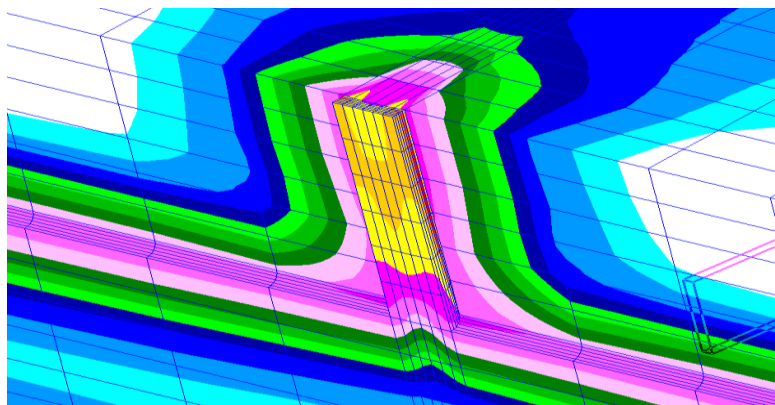

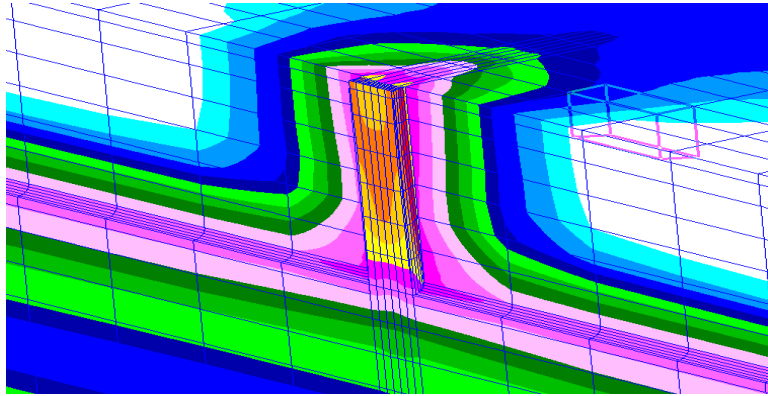**Figure 4.4:** Stress distribution at pressure 20 MPa.

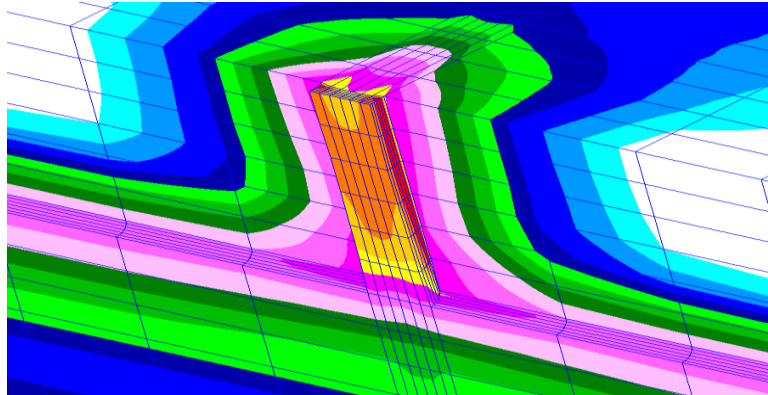**Figure 4.5:** Stress distribution at pressure 27.3 MPa.

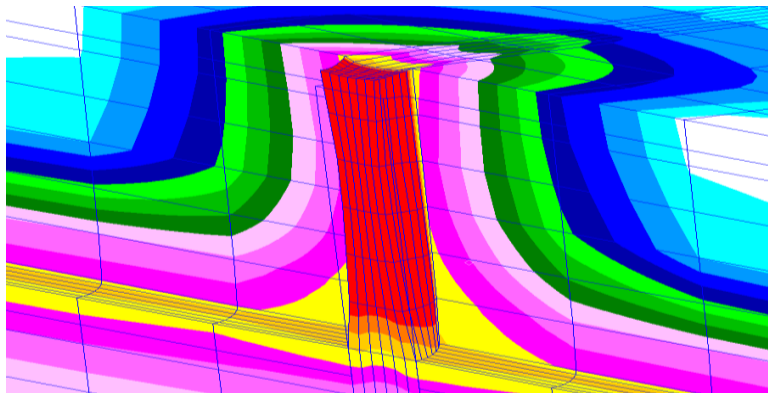**Figure 4.6:** Stress distribution at pressure 30 MPa.

Figure 4.7: Stress distribution at pressure 35 MPa.

To compare the different of the distance between cracks, Case 14 was referred where the length of the crack for both left and right is 100 mm while the distance between the cracks is increased to 2 mm are shown in Figure 4.9. In this case, the pipe was failed at 40.5 MPa is shown in Figure 4.13. The stress concentrations are still higher at both ends of the distance between the cracks that is at 0 mm and 2 mm while stresses are reduced as they approach the centre of the distance between the cracks. This can be seen from Figure 4.10 until Figure 4.12. For pressure at 45 MPa the von Mises stress along the distance between the cracks are all equal to 579 MPa are shown in Figure 4.14. The maximum pressure for this defect is at 40.5 MPa where the stress is exceeding the ultimate tensile stress.
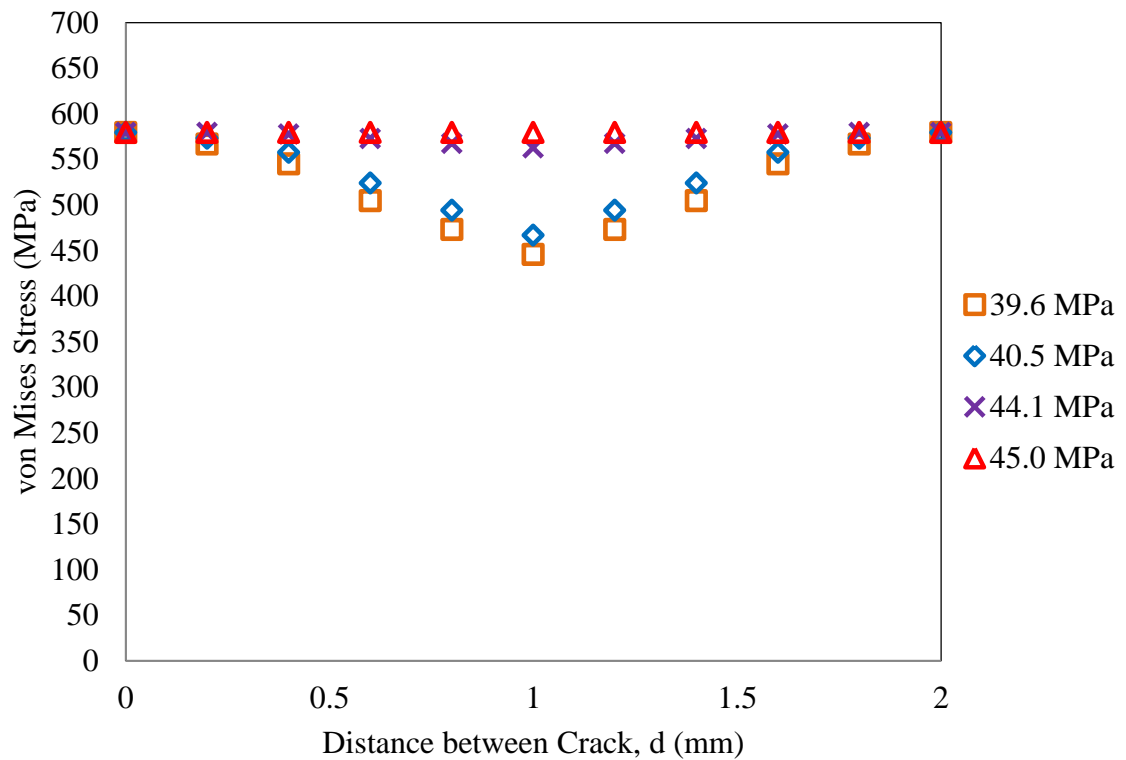
Figure 4.8: Graph Von Mises stress versus distance between cracks for Case 14.

Figure 4.9: Stress distribution at pressure 0 MPa.

Figure 4.10: Stress distribution at pressure 10 MPa.

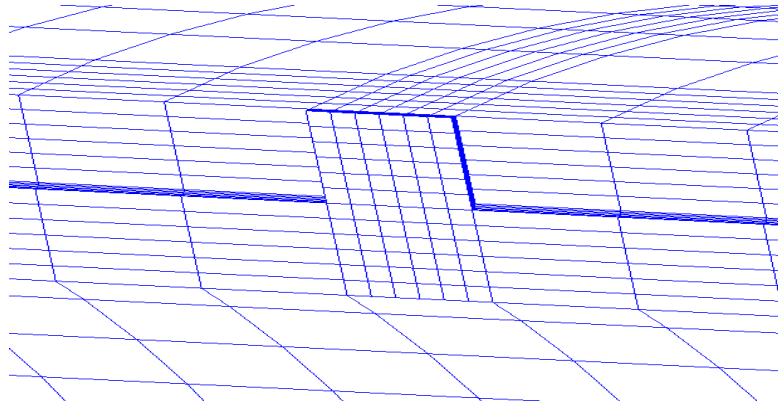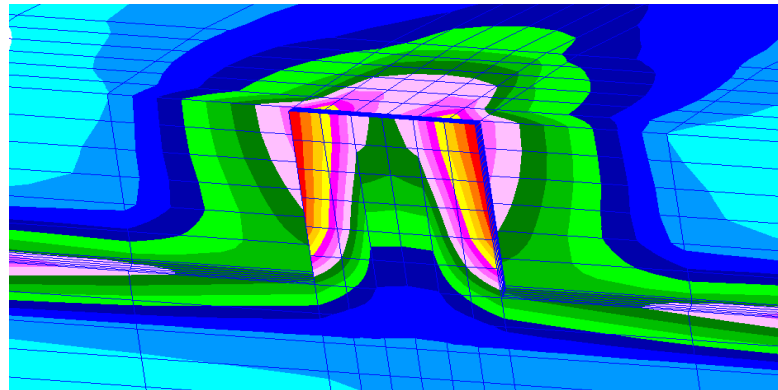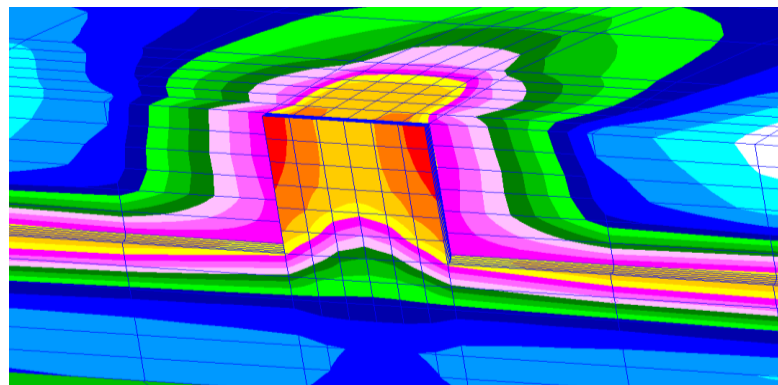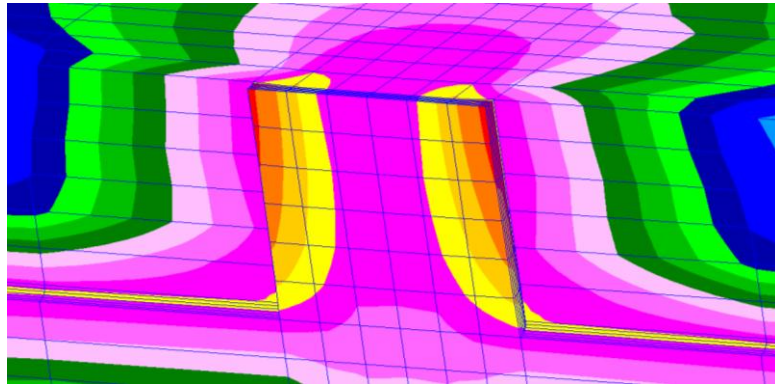**Figure 4.11:** Stress distribution at pressure 20 MPa.

Figure 4.12: Stress distribution at pressure 30 MPa.
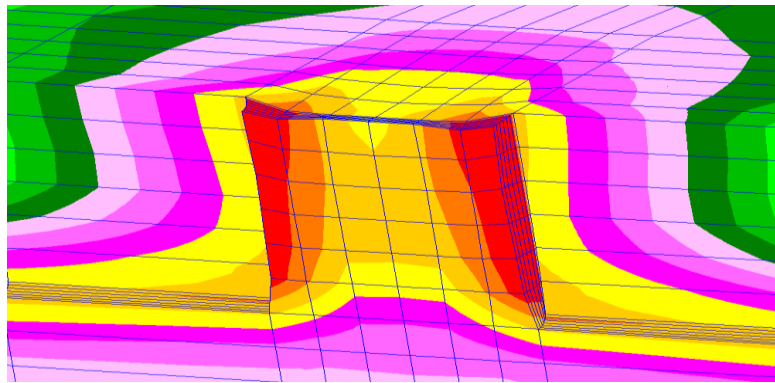
Figure 4.13: Stress distribution at pressure 40.5 MPa.
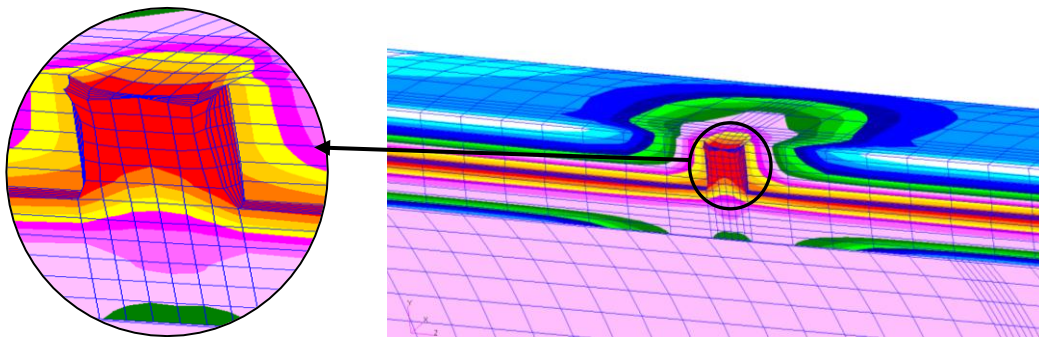
Figure 4.14: Stress distribution at pressure 45 MPa.

For both comparison between Case 13 and Case 14, the stress distribution are higher at both ends of the distance between cracks. The Figures 4.9 until Figure 4.14 also show the stress start to propagate from the tip of the crack which then becomes higher compare to the stress at the center of the distance between cracks. Besides that, there is an interaction of the distance between cracks as it structure were disturbed by the increasing of the pressure apply.

Table 4.1 shows the summarization of the prediction of failure pressure for each case. From the Table 4.1 the data show the pressures are kept increasing as the distances between the cracks become larger.

Table 4.1: Pressure result from the FEA.

Type of case	Crack length 2c (mm)	Distance between, d crack (mm)	Pressure, P (MPa)
Case 1	25	0.5	31.00
Case 2		2	43.40
Case 3		4	46.40
Case 4		8	52.80
Case 5	50	0.5	28.00
Case 6		2	41.04
Case 7		4	44.20
Case 8		8	49.90
Case 9	75	0.5	27.00
Case 10		2	41.00
Case 11		4	44.00
Case 12		8	49.50
Case 13	100	0.5	27.30
Case 14		2	40.50
Case 15		4	41.40
Case 16		8	48.40

4.2.2 Variation of Pressure and Crack Length.

Figure 4.15 shows the pressure that predicted as the failure pressure of the pipe due to the differences of crack length. This data was taken from the simulation by selecting the distance between cracks and the pressure is represented the failure pressure estimation when the von Mises stress at the distance between cracks reaches the ultimate tensile stress.

The graph in Figure 4.15 shows the pressure increase as the distance between crack increases from 0.5 mm to 8 mm for each crack length. At distance between cracks equal to 0.5 mm the pressure decrease as the crack length increase from 25 mm to 100 mm. This is also occurred similar to the other distance between cracks at 2 mm to 8 mm. Besides that, the different of pressure between 0.5 mm to 2 mm distance between cracks is very large compare the different of pressure between 2 mm to 4 mm, and 4 mm to 8 mm. This occur because of the distance between cracks is increase four times from 0.5 mm to 2 mm. The pressure different between 2 mm to 4 mm are small because the interaction of the cracks exist and it is show that at the crack length 100 mm the pressure almost the same at 40 MPa. The pressures are keep increase as the distance between cracks increase. This can be seen from the 4 mm to 8 mm distance between cracks. As the crack length increase the burst pressure sees to reach constant value which the crack length is not the major effect of the burst pressure.
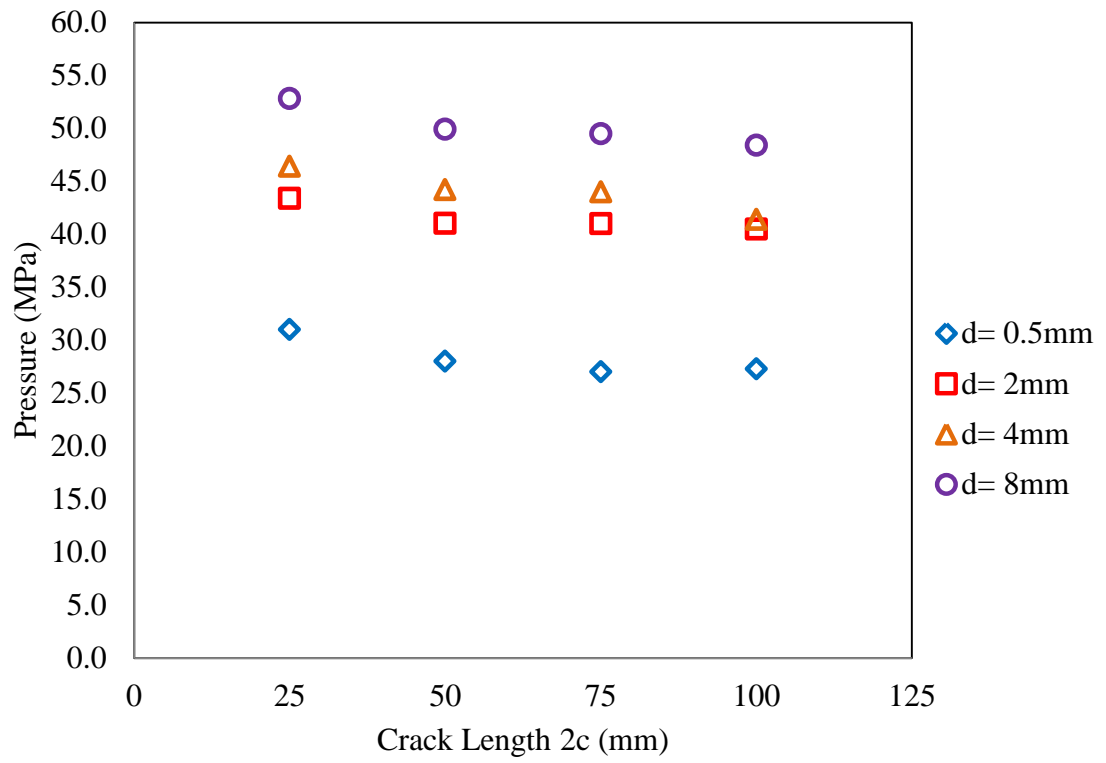
Figure 4.15: Graph pressure versus crack length.

4.2.3 Distance between Cracks and Pressure.

Figure 4.16 shows the graph for the distance between the crack and the estimation failure pressure resulting from FEA simulation. The graph above shows the behaviour of the pressure when the distance between the cracks is maintained while the crack length is varied for 25 mm, 50 mm, 75 mm, and 100 mm.

For the distance between crack equal to 0.5 mm, the pressure for Case 1 is higher that is 31.0 MPa compare to Case 13 which is 27.3 MPa. There is only a slightly different in pressure for the Case 5 and Case 9 which are 28.0 MPa and 27.0 MPa respectively. This comparison is referring the same distance between cracks for each case but the length is varied. From this comparison it shows the pressure decrease as the crack length increase with the same distance between cracks.

For the distance between crack is 2 mm, the comparison of the pressure is made between Case 2, Case 6, Case 10, and Case 14. The result shows the pressure for Case 2 is higher than other cases that 43.3 MPa while the lowest pressure is 40.5 MPa for Case 14. There is no significant difference in pressure for Case 6 and Case 10 is at 41.4 MPa and 41.0 MPa. From both 0.5 mm and the 2 mm distance between cracks the estimation failure pressure is decrease as the cracks length are getting further away.

At a 4 mm distance between the cracks, the lower pressure is for Case 15 and the higher pressure is for Case 3 which is 41.4 MPa and 46.4 MPa respectively. This can be seen from plotted graph at the point for Case 15 and Case 3 are quite far so that show a significant difference in pressure. For Case 11 and Case 7, the pressure differentials are small as it shows the pressure in both cases is almost the same

From the graph above, the behavior of the failure pressure can be estimate increasing as the distance between the cracks become larger. The trends for pressure are almost the same for the distance between crack 0.5 mm, 2 mm, 4 mm and 8 mm. This

show the distance between the cracks play important role in reducing or increasing the failure pressure.
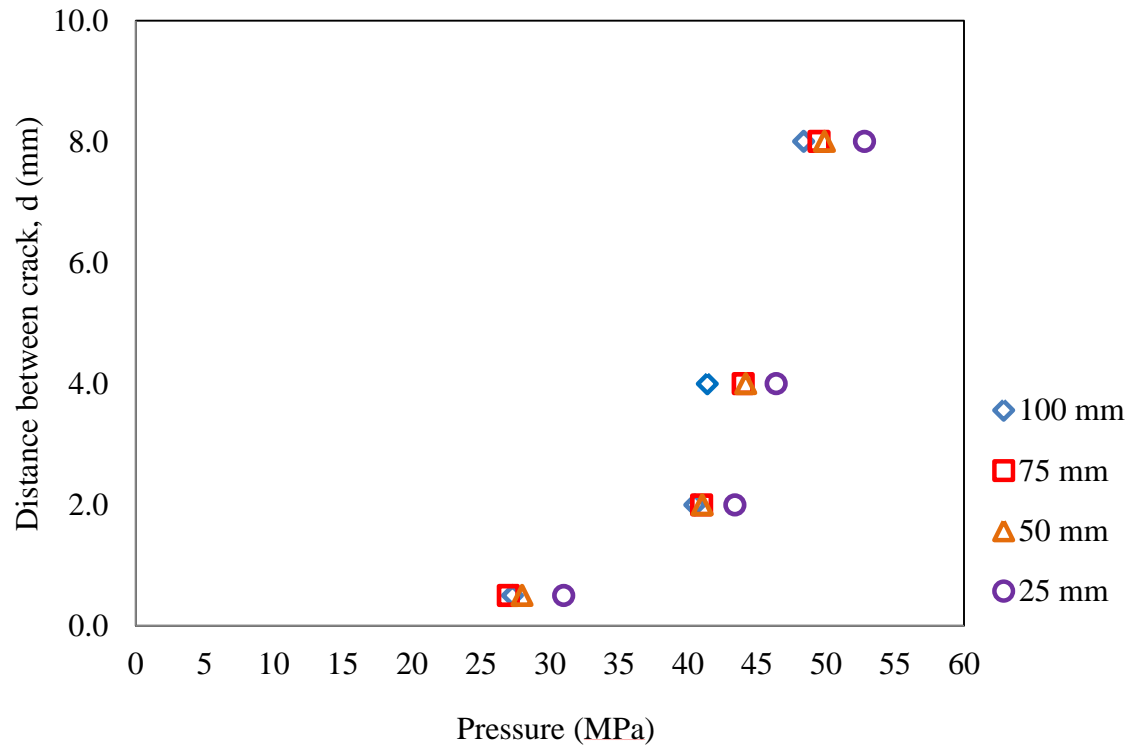

Figure 4.16: Graph pressure versus distance between cracks.

4.2.4 Comparison Industry Models with FEA Result.

Figure 4.17 shows the burst pressure calculated using burst pressure codes such ASME B31G, Modified ASME, and DNV predict the early failure of the defect pipe. The equation used for ASME B31G, Modified ASME and DNV are from Equation (2.1), (2.4) and (2.7) respectively. Recently developed methods such as DNV-RP-F101 are based on equations fitted to the results of a large number of finite element analyses of blunt, part wall defects, these analyses incorporated a failure criterion validated against actual burst tests. The DNV-RP-F101 method was developed to be mean fits to the experimental and numerical data, and so should be the most accurate methods. The modified B31G method is more accurate than the original ASME B31G method.

From the above graph show the result of the 0.5 mm distance between cracks which are from Case 1, Case 5, Case 9, and Case 13. The burst pressure codes calculation is to be compared with the FEA result. Pressure for the Case 1 and Case 9 calculate using ASME B31G code are higher than the FEA pressure result while using DNV code the pressure is higher in all cases. This because DNV code is use ultimate tensile stress in the calculation for predicting the burst pressure compare to the other codes used yield stress for their estimation in failure pressure. For Modified ASME code, it is clearly showing the increment in pressure as the crack length increase from 25 mm to 100 mm whereas for ASME B31G code show the constant pressure at 24.0 MPa for all cases except for crack length 25 mm the pressure are quite high at 35.0 MPa. Besides that, the cases that have pressure that exceed the FEA result are too much higher to be referred as burst pressure because the codes only have a single crack length parameter. Moreover, the cases that have the pressure below the FEA result can be predicted as the burst pressure because the burst pressure is higher for single crack compare to two cracks with same crack length.
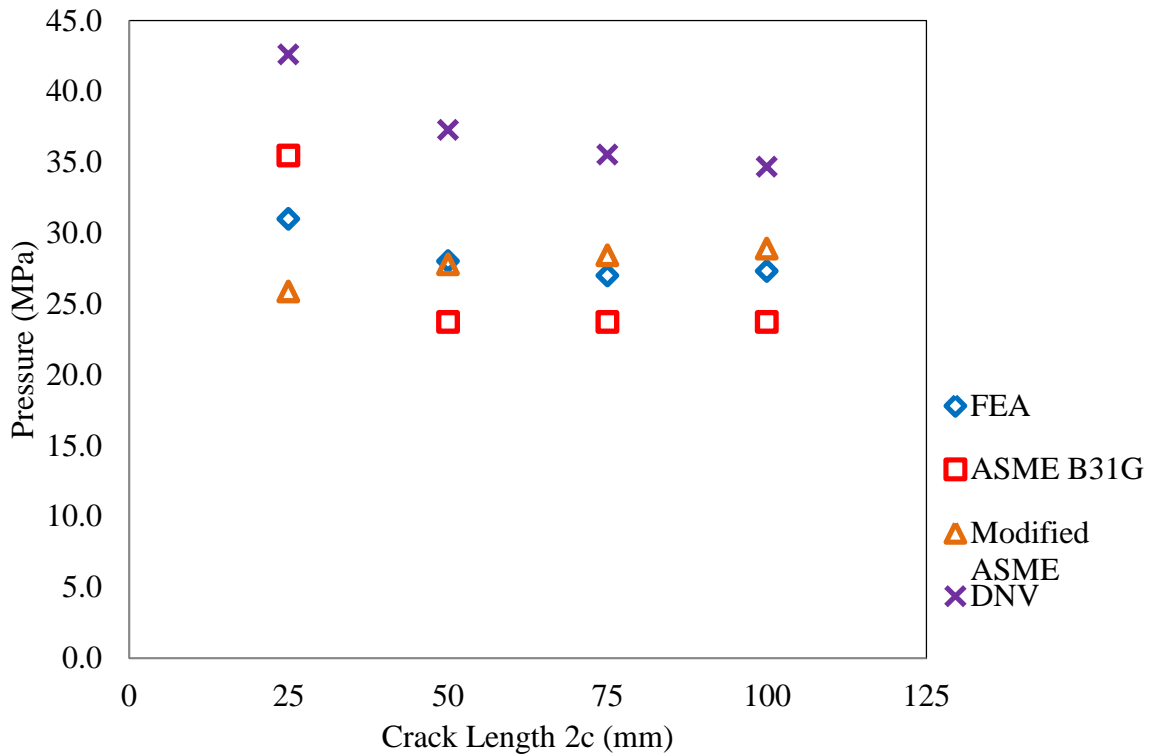
Figure 4.17: Graph pressure versus crack length for 0.5 mm distance between the cracks.

Figure 4.18 shows the graph for the 2 mm distance between cracks which are from Case 2, Case 5, Case 10, and Case 14. From the graph above, pressure for all cases that calculated using ASME B31G, Modified B31G, and DNV code are below than the FEA pressure result. For Modified ASME code, there is an increment in pressure as the crack length increase from 25 mm to 100 mm whereas for ASME B31G code show the constant pressure at 24.0 MPa for all cases except for crack length 25 mm the pressure are quite high at 35.0 MPa. Moreover, the graph show the pressure from DNV code is almost nearly the FEA result compares to other codes and this analysis results would be much reliable to predict the early failure of the defect pipe because FEA is an acceptable tool to analyse the burst pressure. Figure 4.19 and Figure 4.20 show the pressure versus crack length for 4 mm and 8 mm distance between the cracks. The behavior of those plotted graph are same as Figure 4.18.
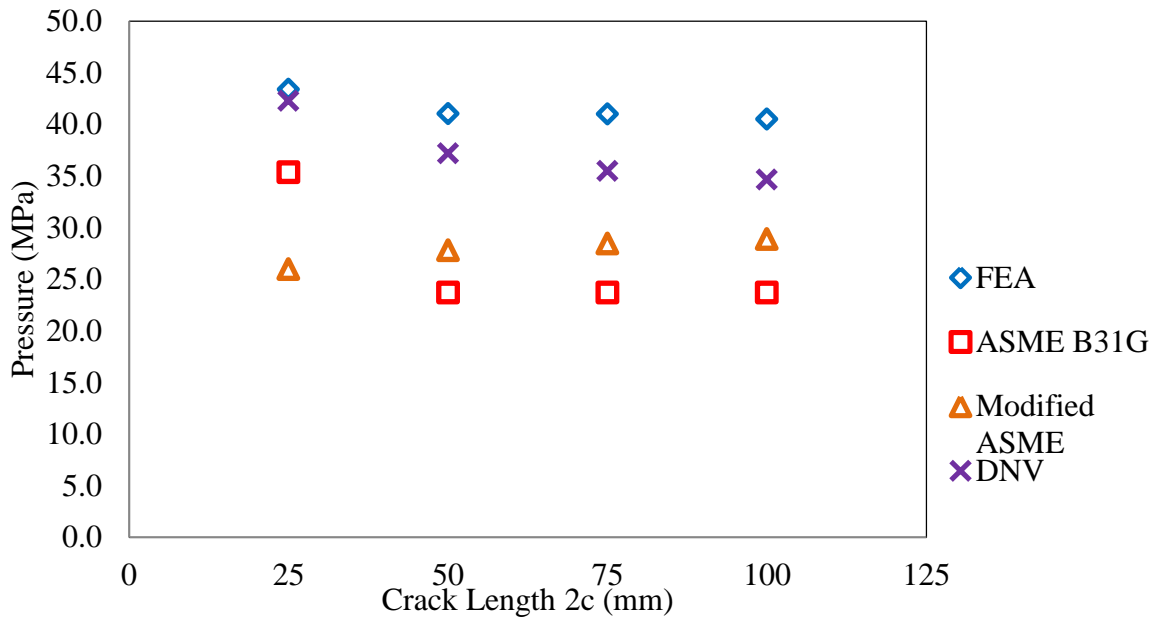
Figure 4.18: Graph pressure versus crack length for 2 mm distance between the cracks.
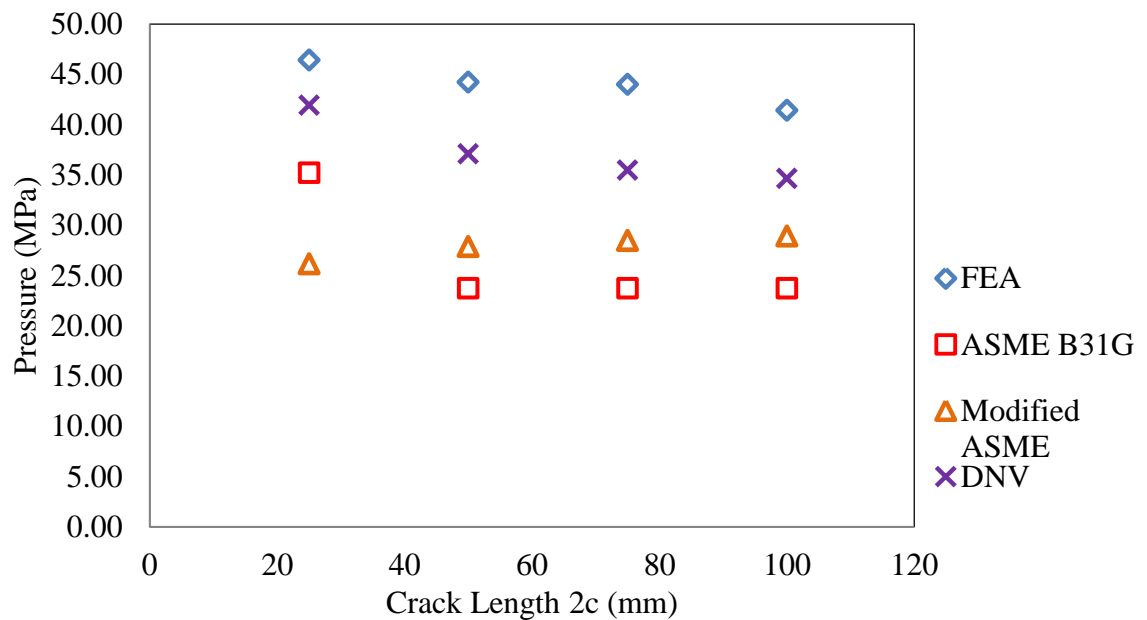

Figure 4.19: Graph pressure versus crack length for 4 mm distance between the cracks.
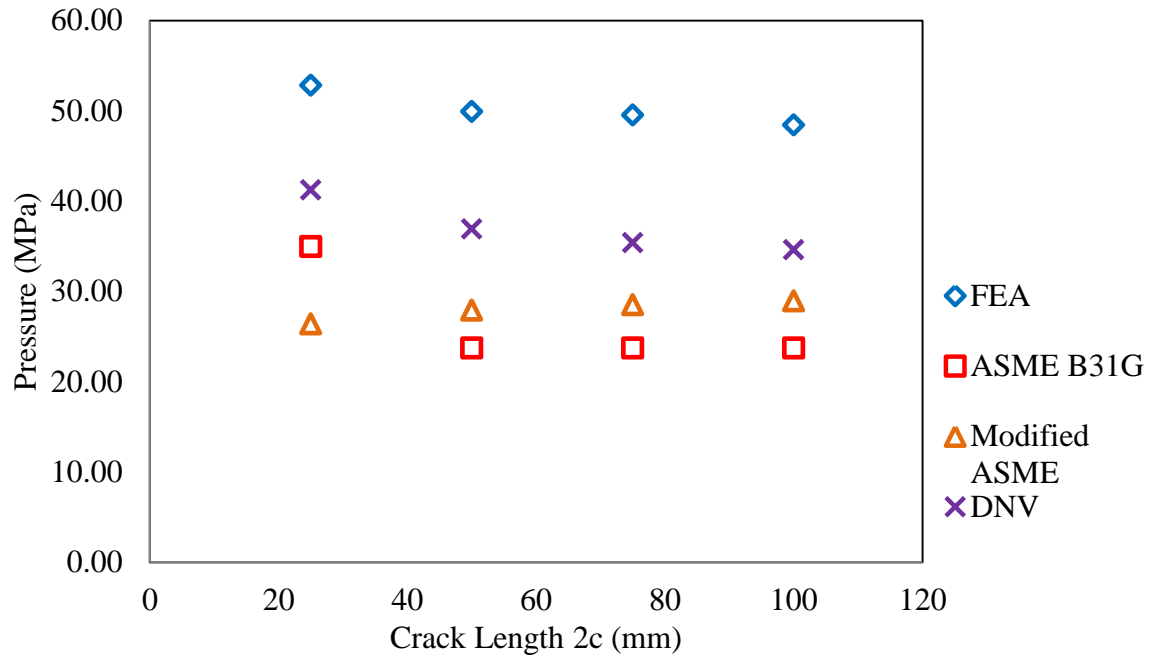
Figure 4.20: Graph pressure versus crack length for 8 mm distance between the cracks.

4.2.5 Displacement at Z Axis

Figure 4.21 show the sketch of the defect pipe model. The length of the pipe and crack length is along the z axis direction while the thickness is in the y axis direction. Figure 4.22 show the displacement and the distance between cracks 0.5 mm from Case 1, Case 5, Case 9, and Case 13. It is shown the displacement occurs from both ends of the distance between the cracks. The displacement is decreasing from 0.008 mm at the right end of 0.001 mm at the centre of the distance between the cracks. The other side also shows the same decrement in length as the crack length from both right and left of the distance between the cracks is in the same size. From the bar chart in Figure 4.23 show the percentage of the remaining distance after the displacement occurs. There is almost 6 % of the distance between cracks have deform from the actual length. These trends are almost the same in every case that have been analysed. This result shows that the failures of the pipe have no significant effect in the deformation of the distance between the cracks.

Figure 4.21: The z axis direction.

Figure 4.22: Graph displacement versus 0.5 mm distance between cracks.
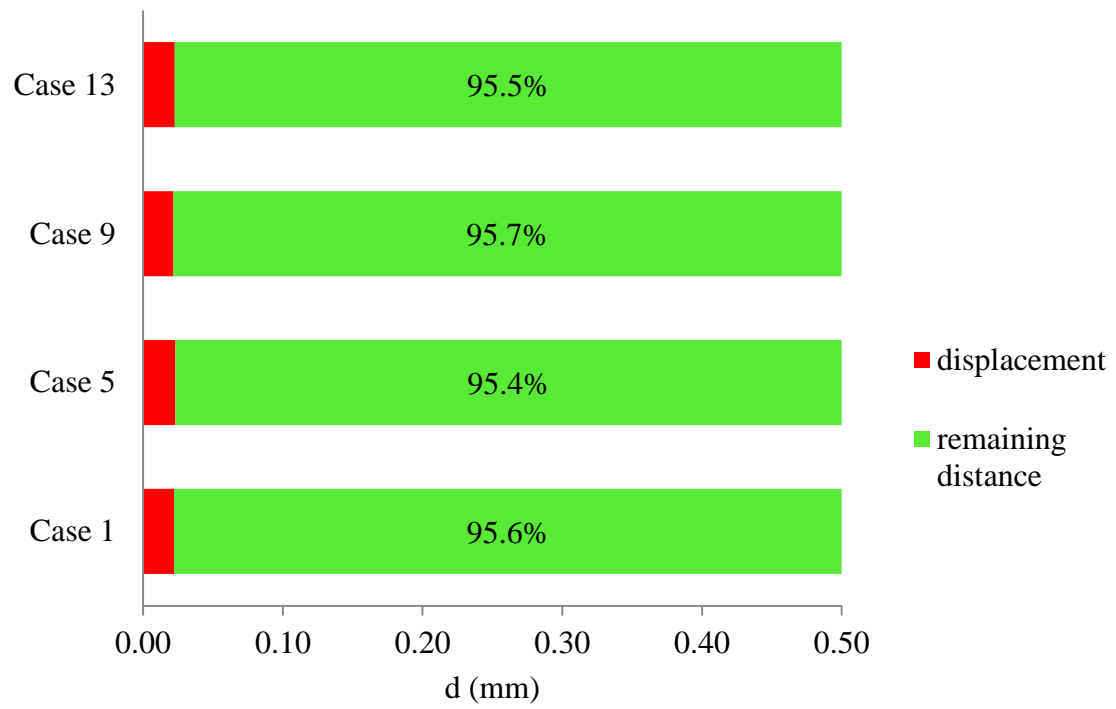
Figure 4.23: Displacement and remaining distance between cracks for 0.5 mm.

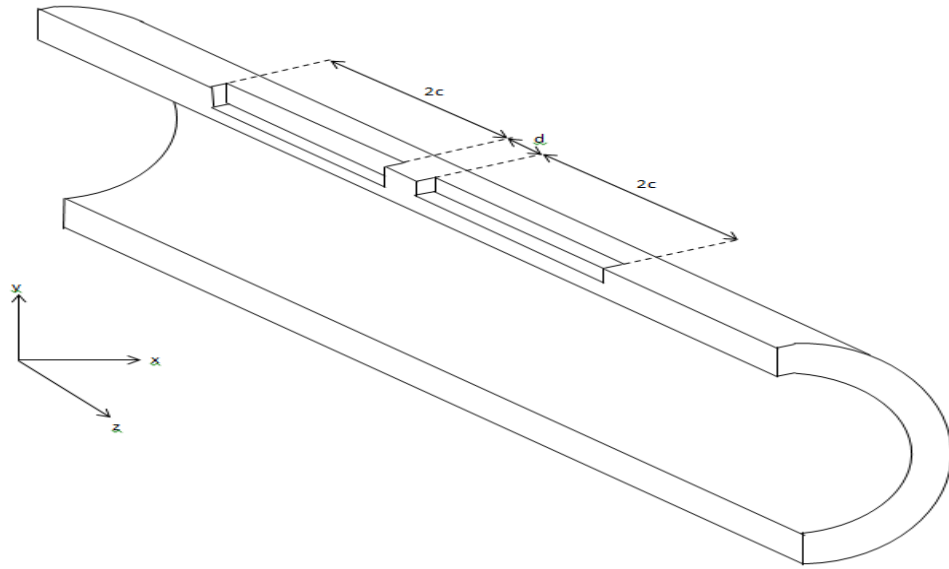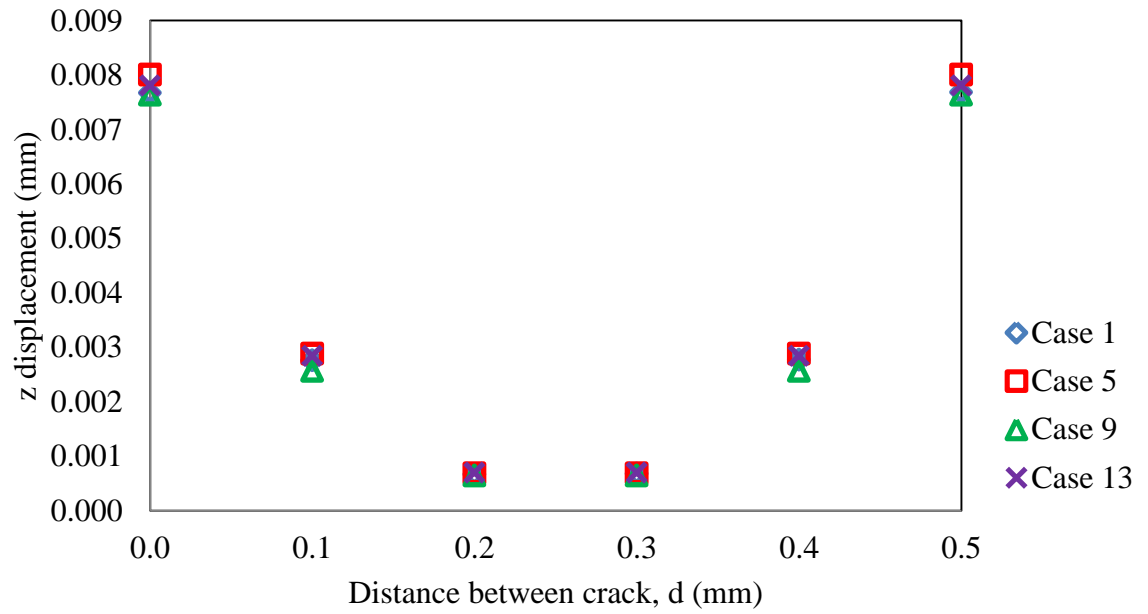# CHAPTER 5

CONCLUSION AND RECOMMENDATIONS

5.1 INTRODUCTION

This chapter will conclude the analysis project and briefly discussed about the recommendation that can apply in the future work. The conclusion were done according to the result obtain in Chapter 4. In order to study the crack interaction using FEA, other aspects of future work also will be discussed.

5.2 CONCLUSION

In this study, the first objective is to analyze the maximum pressure for various crack distance and crack length. The second objective is to study about the interaction between two cracks in a pipeline.

From the result in Chapter 4, the interaction of the stress occurs at both ends of the distance between cracks. Those stresses start to concentrate at both ends of the distance between the cracks which are higher than the stress at the centre of the distance between cracks. The stresses at the cracks distribute equally then they are concentrating at the ends of crack thus cause the stress interaction. The stresses are becoming smaller as they approach the centre of the distance between cracks because the pressure apply are not yet affect stress concentration at that point. But if the pressure keeps increasing the stress at the centre of distance between cracks become higher thus try to connect the high stress concentration from both ends.

Besides that, the maximum pressure resulting from the FEA simulation was predicted as the failure pressure or the burst pressure for the pipe because the stress where the concentration of the stress higher has reached the ultimate tensile strength. For the distance between cracks, the estimation of the failure pressure has increase as the distance between the cracks are getting further away. Moreover, the failure pressure also has been estimated increase as the cracks length becomes larger. This show the distance between the cracks and the crack length play important role in estimating the failure pressure of the defect pipe.

5.3 RECOMMENDATIONS

The recommendation is very necessary in this project because it will affect the quality of the project in the future. This recommendation part is a suitable medium to give an opinion, suggestions or ideas about the improvement and enhance the project management as well as the data collection. For the sake of this study, weakness and disadvantage of this project must be overcome and so the quality of the future study would be much better.

Firstly, in the meshing process by using MSC Patran 2008 r1 software must be done properly because the simple or complicated mesh for the simulation will be affect the result. It also includes the number of mesh and element, type of mesh and how to mesh correctly also the factor in getting the accurate result. Besides, for a good result the study area or the interest region should have more focus mesh. So, careful with the meshing and make sure the meshing becomes smooth and proper for the best result.

Secondly, the type material used for this project should be varied. There are many types or standard of the pipeline used out there for oil and gas transmission. Different pipe standard have the different mechanical properties as well as chemical composition can be used for the simulation for this project. For example the materials used have to be in various types of API steel such as API X65, API X70, and API X100. It should compare with the different pipeline standard to get the best type of pipe

selection for the real situation. The case study of the project also can be broad as the data from the analysis is not limited to one type of pipe.

In addition, a few experiments should be carried out to predict the burst pressure. Experimental results should be compared to the FEA results. The percentage of error for analysis can be calculated for comparison between the experimental results and the finite element results.

Lastly, the use of several FEA softwares should be used in this project to get accurate results and all the data can be compared and review in detail because the different software has a different method of completion.

REFERENCES

ANSI/API Specification 5L, Specification for Line Pipe**.** Forty-Fourth Edition, October 1, 2007

Ashby, M.F. and Johnson, K. 2009. *Materials and design: the art and science of material selection in product design*. Butterworth-Heinemann.

Beavers, J.A. and Thompson, N.G. 2006."External Corrosion of Oil and Natural Gas Pipelines". *ASM International*.**13C**.

Belachew C. T., Mokhtar C. Ismail, and Saravanan K. 2009. Evaluation Of Available Codes For Capacity Assessment Of Corroded Pipelines. Universiti Teknologi Petronas, Mechanical Engineering DepartmentBandar Sri Iskandar, 31750 Tronoh,

Bennett, D.C. 2002. Corrosion damage mechanisms and their prevention in tanks containing alkaline pulping liquors*. Tappi Fall Conference & Trade Fair*.

Budynas, R.G. and Nisbett, J.K. 2011.*Shigley's Mechanical Engineering Design*. Ninth Edition In SI Units. New York: McGraw-Hill.

Efunda, Inc. 2012. Electronic sources: Failure Criteria: Ductile Materials. http://www.efunda.com/formulae/solid_mechanics/failure_criteria/failure_criteria_ductile.cfm

Iversen, A. and Leffler, B. 2010. Aqueous corrosion of stainless steel. *Ferrous Metal and Alloys*. 1806-1877.

Kadhim, F.S. 2011. Investigation of carbon steel corrosion in water base drilling mud. *Modern Applied Science*. **5**(1): 224-229.

Kim, W.K., Jung, H.G. and Koh, K.Y. 2008. The Effect of Metallurgical Factors on SOHIC in HIC Free Linepipe Steels. *The International Society of Offshore and Polar Engineers*. 978-1-880653

L.Y. Xu and Y.F. Cheng. 2012. Reliability and failure pressure prediction of various grades of pipeline steel in the presence of corrosion defects and pre-strain. *International Journal of Pressure Vessels and Piping*. **89**. 75-84.

Morrow, S.J. 2010. Materials selection for seawater pumps. *Proceedings of the Twenty sixth International Pump Users Symposium*. 73-80.

W. Zhou, G.X. Huang. 2012. Model error assessments of burst capacity models for corroded pipelines. *International Journal of Pressure Vessels and Piping.* (99-100): 1-8

Y.K Lee, Y.P. Kim, M.W. Moon, W.H. Bang, K.H. Oh, W.S. Kim. 2005. The prediction of failure pressure of gas pipeline with multi corroded region. *Material Science forum.* 475-479

Task		Week													
		1	2	3	4	5	6	7	8	9	10	11	12	13	14
FYP title discussion	P	■													
	A	▨													
Scopes and Objectives	P		■	■											
	A		▨	▨											
Gantt Chart and Flow Chart propose	P			■											
	A			▨											
Prepare Introduction	P			■	■	■									
	A				▨	▨	▨								
Find Literature Review	P				■	■	■	■	■	■	■				
	A					▨	▨	▨	▨	▨	▨				
Learn MSC Software	P					■	■	■	■	■	■	■			
	A					▨	▨	▨	▨	▨	▨	▨	▨		
Determine Methodology	P										■	■	■		
	A										▨	▨	▨		
Present to Supervisor (midsem)	P							■							
	A							▨							
Submit report and log book	P													■	
	A													▨	
FYP1 Presentation	P														■
	A														▨

P = planning

A = actual

Figure A: Project planning (Gantt chart) final year project 1.

Task		Week														
		1	2	3	4	5	6	7	8	9	10	11	12	13	14	15
Scheduling task	P	■														
	A	■														
Consult with Supervisor	P		■													
	A		■													
Run Simulation	P	■	■	■	■	■	■	■	■							
	A	■	■	■	■	■	■	■	■	■						
Collecting data	P		■	■	■	■	■	■	■							
	A		■	■	■	■	■	■	■	■						
Analyze data	P				■	■	■	■	■	■						
	A	■	■	■	■	■	■	■	■	■						
Result discussion and report writing	P						■	■	■	■	■	■				
	A						■	■	■	■	■	■	■	■		
Writing abstract and conclusion	P											■	■			
	A											■	■			
Present to Supervisor (midsem)	P						■									
	A						■									
Submit final report	P														■	
	A														■	
FYP Presentation	P														■	
	A															■

P = planning

A = actual

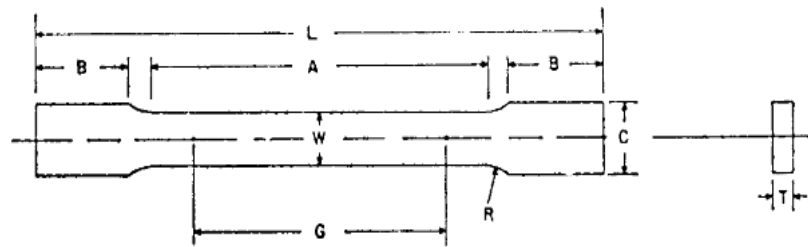Figure B: Project planning (Gantt chart) final year project 2.

APPENDIX D

Dimensions

	Standard Specimens		Subsize Specimen
	Plate-Type, 1½-in. Wide	Sheet-Type, ½-in. Wide	¼-in. Wide
	in.	in.	in.
G—Gage length (Note 1 and Note 2)	8.00± 0.01	2.000± 0.005	1.000 ± 0.003
W—Width (Note 3 and Note 4)	1½ + ⅛, − ¼	0.500± 0.010	0.250 ± 0.005
T—Thickness (Note 5)		thickness of material	
R—Radius of fillet, min (Note 6)	1	½	¼
L—Over-all length, (Note 2, Note 7 and Note 8)	18	8	4
A—Length of reduced section, min	9	2¼	1¼
B—Length of grip section, (Note 8)	3	2	1¼
C—Width of grip section, approximate (Note 4 and Note 9)	2	¾	⅜

Figure D: The standard ASTM tensile test dimension for plane specimen.

FOUNDRY LABORATORY
FACULTY OF MECHANICAL ENGINEERING
UNIVERSITI MALAYSIA PAHANG

Chemical Results   Date: 11/03/2013

Sample ID: Material: steel pipe
Customer: Alif   Dimension:
Commision: Filter metals:
Lab-no.:   Heat treatment:
Reference no.:   Heat-no:

Spectrometer Foundry-MASTER   Grade :

	Fe	C	Si	Mn	P	S	Cr	Mo	Ni	Cu
1	98.5	0.267	0.354	0.564	< 0.010	< 0.010	0.0285	< 0.010	0.0174	< 0.005
2	98.8	0.249	0.288	0.552	< 0.010	< 0.010	0.0247	< 0.010	0.0117	< 0.005
3	98.8	0.257	0.286	0.562	< 0.010	< 0.010	0.0264	< 0.010	0.0132	< 0.005
Ave	98.7	0.258	0.309	0.559	< 0.010	< 0.010	0.0265	< 0.010	0.0141	< 0.005

Foundry Laboratory   Test by: Verify by:
Faculty of Mechanical Engineering
Universiti Malaysia Pahang
26600 Pekan, Pahang, MALAYSIA
Tel: +604242213 / 2270 / 2317
Fax: +6094242202
Website: http//:fkm.ump.edu.my